Inorganic Chemistry
Article

Inorg. Chem. **2011**, *50*, 1123–1134 **1123**
DOI: 10.1021/ic1020059

Toward the Self-Assembly of Metal−Organic Nanotubes Using Metal−Metal and π-Stacking Interactions: Bis(pyridylethynyl) Silver(I) Metallo-macrocycles and Coordination Polymers

Kelly J. Kilpin,[†] Martin L. Gower,[†] Shane G. Telfer,[‡,§] Geoffrey B. Jameson,[‡] and James D. Crowley*[,†]

[†]*Department of Chemistry, University of Otago, P.O. Box 56, Dunedin, New Zealand,* [‡]*Institute of Fundamental Sciences, Massey University, Private Bag 11 222, Palmerston North, New Zealand, and* [§]*MacDiarmid Institute for Advanced Materials and Nanotechnology, Wellington, New Zealand*

Received September 30, 2010

Shape-persistent macrocycles and planar organometallic complexes are beginning to show considerable promise as building blocks for the self-assembly of a variety of supramolecular materials including nanofibers, nanowires, and liquid crystals. Here we report the synthesis and characterization of a family of planar di- and tri-silver(I) containing metallo-macrocycles designed to self-assemble into novel metal−organic nanotubes through a combination of π-stacking and metal−metal interactions. The silver(I) complexes have been fully characterized by elemental analysis, high resolution electrospray ionization mass spectrometry (HR-ESI-MS), IR, ^{1}H and ^{13}C NMR spectroscopy, and the solution data are consistent with the formation of the metallo-macrocycles. Four of the complexes have been structurally characterized using X-ray crystallography. However, only the di-silver(I) complex formed with 1,3-bis(pyridin-3-ylethynyl)benzene is found to maintain its macrocyclic structure in the solid state. The di-silver(I) shape-persistent macrocycle assembles into a nanoporous chicken-wire like structure, and ClO_4^- anions and disordered H_2O molecules fill the pores. The silver(I) complexes of 2,6-bis(pyridin-3-ylethynyl)pyridine and 1,4-di(3-pyridyl)buta-1,3-diyne ring-open and crystallize as non-porous coordination polymers.

Introduction

Nature exploits noncovalent forces such as hydrogen bonding, hydrophobic, dipole−dipole, and van der Waals interactions to self-assemble a vast range of functional molecular architectures from a small set of relatively "simple" building blocks. Inspired by this, the use of self-assembly as an approach for the generation of ordered nanoscale structures and (supra)molecule-based devices has engendered considerable attention in the materials sciences.[1] Shape-persistent macrocycles (SPMs)[2] are one class of molecules that have been extensively examined in this regard. The rigid macrocyclic framework of SPMs has been exploited as a building block for the generation of a variety of supramolecular assemblies including host−guest complexes,[3] discotic liquid crystals,[2] sensors,[4] nanotubes[5] and nanofibers,[4,6] and organic porous solids.[7] These supramolecular systems usually exploit either $\pi-\pi$ interactions or hydrogen-bonding interactions in the assembly process.[2,6,8]

Recently, planar organometallic complexes have also begun to show promise as building blocks for the construction of self-assembled nanoscale materials.[9] In particular, the synthesis of planar platinum(II) or gold(I) complexes containing

*To whom correspondence should be addressed. E-mail: jcrowley@chemistry.otago.ac.nz. Fax: +64 3 479 7906. Phone: +64 3 479 7731.

(1) For recent reviews see: Hui, J. K. H.; MacLachlan, M. J. *Coord. Chem. Rev.* **2010**, *254*, 2363–2390. Ferey, G. *Chem. Soc. Rev.* **2008**, *37*, 191–214. Ferey, G. *Dalton Trans.* **2009**, 4400–4415. Dinca, M.; Long, J. R. *Angew. Chem., Int. Ed.* **2008**, *47*, 6766–6779. Murray, L. J.; Dinca, M.; Long, J. R. *Chem. Soc. Rev.* **2009**, *38*, 1294–1314. Roy, X.; MacLachlan, M. J. *Chem.—Eur. J.* **2009**, *15*, 6552–6559. Rowsell, J. L. C.; Yaghi, O. M. *Microporous Mesoporous Mater.* **2004**, *73*, 3–14. Whitesides, G. M. *Small* **2005**, *1*, 172–179. Palmer, L. C.; Stupp, S. I. *Acc. Chem. Res.* **2008**, *41*, 1674–1684.

(2) Hoeger, S. *Pure Appl. Chem.* **2010**, *82*, 821–830. Zhang, W.; Moore, J. S. *Angew. Chem., Int. Ed.* **2006**, *45*, 4416–4439. MacLachlan, M. J. *Pure Appl. Chem.* **2006**, *78*, 873–888. Hoeger, S. *Chem.—Eur. J.* **2004**, *10*, 1320–1329. Zhao, D.; Moore, J. S. *Chem. Commun.* **2003**, 807–818.

(3) Hua, Y.; Flood, A. H. *Chem. Soc. Rev.* **2010**, *39*, 1262–1271.

(4) Balakrishnan, K.; Datar, A.; Zhang, W.; Yang, X.; Naddo, T.; Huang, J.; Zuo, J.; Yen, M.; Moore, J. S.; Zang, L. *J. Am. Chem. Soc.* **2006**, *128*, 6576–6577.

(5) Tian, L.-l.; Wang, C.; Dawn, S.; Smith, M. D.; Krause, J. A.; Shimizu, L. S. *J. Am. Chem. Soc.* **2009**, *131*, 17620–17629. Yang, J.; Dewal, M. B.; Sobransingh, D.; Smith, M. D.; Xu, Y.; Shimizu, L. S. *J. Org. Chem.* **2009**, *74*, 102–110. Xu, Y.; Smith, M. D.; Geer, M. F.; Pellechia, P. J.; Brown, J. C.; Wibowo, A. C.; Shimizu, L. S. *J. Am. Chem. Soc.* **2010**, *132*, 5334–5335.

(6) Zang, L.; Che, Y.; Moore, J. S. *Acc. Chem. Res.* **2008**, *41*, 1596–1608.

(7) Venkataraman, D.; Lee, S.; Zhang, J.; Moore, J. S. *Nature* **1994**, *371*, 591–593.

(8) Pasini, D.; Ricci, M. *Curr. Org. Synth.* **2007**, *4*, 59–80. Hoeger, S. *Angew. Chem., Int. Ed.* **2005**, *44*, 3806–3808.

(9) Elemans, J. A. A. W.; van Hameren, R.; Nolte, R. J. M.; Rowan, A. E. *Adv. Mater.* (*Weinheim, Ger.*) **2006**, *18*, 1251–1266. Hoeben, F. J. M.; Jonkheijm, P.; Meijer, E. W.; Schenning, A. P. H. J. *Chem. Rev.* **2005**, *105*, 1491–1546. Shimizu, T.; Masuda, M.; Minamikawa, H. *Chem. Rev.* **2005**, *105*, 1401–1443. Simpson, C. D.; Wu, J.; Watson, M. D.; Muellen, K. *J. Mater. Chem.* **2004**, *14*, 494–504.

Published on Web 01/05/2011

π-conjugated ligands has received considerable attention because these molecules tend to be air- and water-stable and have the ability to self-assemble through a combination of metal−metal[10] (Pt−Pt[11] or Au−Au[12]) and $\pi-\pi$ interactions. The resulting cofacially stacked molecular aggregates often demonstrate interesting photophysical and photochemical properties due to orbital interactions between the π systems and metal ions of adjacent complexes. Planar gold(I) and platinum(II) building blocks have been used to generate nanostructured materials with semiconducting,[13] liquid crystalline,[14,15] gelating,[15,16] and luminescent[2,8,14,16] properties.

In light of the above work and given the excellent methods for the generation of metal-containing macrocycles[17] it seems somewhat suprising that so little attention[18] has been directed toward the exploitation of metal-containing shape-persistent macrocycles (MSPMs) for the generation of novel self-assembled materials. Inspired by the seminal work of Moore et al. on the self-assembly of planar *m*-phenylene ethynylene macrocycles[7,19] and coupling with our own interests in metal directed self-assemby[20] and metal−metal interactions,[21] we have examined the use of carefully designed planar MSPMs to assemble novel metal organic nanotubes through a combination of π-stacking and metal−metal interactions.

Metallo-macrocycle Design. The metallo-macrocycles, **1** and **2**, have been carefully designed to form planar MSPMs (Scheme 1). Combining the linear two-coordinate preferring metal ions Ag(I)[22] and Au(I)[23] with bis(pyridylethynyl)

(10) Pyykkö, P. *Chem. Rev.* **1997**, *97*, 597–636.

(11) Phillips, V.; Willard, K. J.; Golen, J. A.; Moore, C. J.; Rheingold, A. L.; Doerrer, L. H. *Inorg. Chem.* **2010**, *49*, 9265–9274. Doerrer, L. H. *Dalton Trans.* **2010**, *39*, 3543–3553. Doerrer, L. H. *Comments Inorg. Chem.* **2008**, *29*, 93–127. Anderson, B. M.; Hurst, S. K. *Eur. J. Inorg. Chem.* **2009**, 3041–3054. Connick, W. B.; Marsh, R. E.; Schaefer, W. P.; Gray, H. B. *Inorg. Chem.* **1997**, *36*, 913–922.

(12) Schmidbaur, H.; Schier, A. *Chem. Soc. Rev.* **2008**, *37*, 1931–1951. *Modern Supramolecular Gold Chemistry: Gold-Metal Interactions And Applications*; Laguna, A., Ed.; Wiley-VCH: Weinheim, Germany, 2008; Hutchings, G. J.; Brust, M.; Schmidbaur, H. *Chem. Soc. Rev.* **2008**, *37*, 1759–1765. Schmidbaur, H. *Gold Bull.* **2000**, *33*, 3–10.

(13) Zhang, Y.; Zhang, H.; Mu, X.; Lai, S.-W.; Xu, B.; Tian, W.; Wang, Y.; Che, C.-M. *Chem. Commun.* **2010**, *46*, 7727–7729. Lu, W.; Ng, K.-M.; Che, C.-M. *Chem.—Asian J.* **2009**, *4*, 830–834. Lu, W.; Chen, Y.; Roy, V. A. L.; Chui, S. S.-Y.; Che, C.-M. *Angew. Chem., Int. Ed.* **2009**, *48*, 7621–7625. Yuen, M.-Y.; Roy, V. A. L.; Lu, W.; Kui, S. C. F.; Tong, G. S. M.; So, M.-H.; Chui, S. S.-Y.; Muccini, M.; Ning, J. Q.; Xu, S. J.; Che, C.-M. *Angew. Chem., Int. Ed.* **2008**, *47*, 9895–9899. So, M.-H.; Roy, V. A. L.; Xu, Z.-X.; Chui, S. S.-Y.; Yuen, M.-Y.; Ho, C.-M.; Che, C.-M. *Chem.—Asian J.* **2008**, *3*, 1968–1978. Lu, X.; Yavuz, M. S.; Tuan, H.-Y.; Korgel, B. A.; Xia, Y. *J. Am. Chem. Soc.* **2008**, *130*, 8900–8901. Lu, W.; Chui, S. S.-Y.; Ng, K.-M.; Che, C.-M. *Angew. Chem., Int. Ed.* **2008**, *47*, 4568–4572. Lu, W.; Roy, V. A. L.; Che, C.-M. *Chem. Commun.* **2006**, 3972–3974. Kim, E.-G.; Schmidt, K.; Caseri, W. R.; Kreouzis, T.; Stingelin-Stutzmann, N.; Bredas, J.-L. *Adv. Mater.* (*Weinheim, Ger.*) **2006**, *18*, 2039–2043. Fontana, M.; Caseri, W.; Smith, P. *Platinum Met. Rev.* **2006**, *50*, 112–117. Caseri, W. R.; Chanzy, H. D.; Feldman, K.; Fontana, M.; Smith, P.; Tervoort, T. A.; Goossens, J. G. P.; Meijer, E. W.; Schenning, A. P. H. J.; Dolbnya, I. P.; Debije, M. G.; de Haas, M. P.; Warman, J. M.; van de Craats, A. M.; Friend, R. H.; Sirringhaus, H.; Stutzmann, N. *Adv. Mater.* (*Weinheim, Ger.*) **2003**, *15*, 125–129. Fontana, M.; Chanzy, H.; Caseri, W. R.; Smith, P.; Schenning, A. P. H. J.; Meijer, E. W.; Groehn, F. *Chem. Mater.* **2002**, *14*, 1730–1735. Bremi, J.; Caseri, W.; Smith, P. *J. Mater. Chem.* **2001**, *11*, 2593–2596.

(14) Santoro, A.; Whitwood, A. C.; Williams, J. A. G.; Kozhevnikov, V. N.; Bruce, D. W. *Chem. Mater.* **2009**, *21*, 3871–3882. Coco, S.; Espinet, P. *Gold Chem.* **2009**, 357–396. Arias, J.; Bardaji, M.; Espinet, P.; Folcia, C. L.; Ortega, J.; Etxebarria, J. *Inorg. Chem.* **2009**, *48*, 6205–6210. Kozhevnikov, V. N.; Donnio, B.; Bruce, D. W. *Angew. Chem., Int. Ed.* **2008**, *47*, 6286–6289. Arias, J.; Bardaji, M.; Espinet, P. *Inorg. Chem.* **2008**, *47*, 3559–3567. Ferrer, M.; Mounir, M.; Rodriguez, L.; Rossell, O.; Coco, S.; Gomez-Sal, P.; Martin, A. *J. Organomet. Chem.* **2005**, *690*, 2200–2208.

(15) Camerel, F.; Ziessel, R.; Donnio, B.; Bourgogne, C.; Guillon, D.; Schmutz, M.; Iacovita, C.; Bucher, J.-P. *Angew. Chem., Int. Ed.* **2007**, *46*, 2659–2662.

(16) Tam, A. Y.-Y.; Wong, K. M.-C.; Yam, V. W.-W. *J. Am. Chem. Soc.* **2009**, *131*, 6253–6260. Tam, A. Y.-Y.; Wong, K. M.-C.; Yam, V. W.-W. *Chem.—Eur. J.* **2009**, *15*, 4775–4778. Tam, A. Y.-Y.; Wong, K. M.-C.; Wang, G.; Yam, V. W.-W. *Chem. Commun.* **2007**, 2028–2030. Cardolaccia, T.; Li, Y.; Schanze, K. S. *J. Am. Chem. Soc.* **2008**, *130*, 2535–2545.

(17) Yoshizawa, M.; Klosterman, J. K.; Fujita, M. *Angew. Chem., Int. Ed.* **2009**, *48*, 3418–3438. Glasson, C. R. K.; Lindoy, L. F.; Meehan, G. V. *Coord. Chem. Rev.* **2008**, *252*, 940–963. Dalgarno, S. J.; Power, N. P.; Atwood, J. L. *Coord. Chem. Rev.* **2008**, *252*, 825–841. Northrop, B. H.; Yang, H.-B.; Stang, P. J. *Chem. Commun.* **2008**, 5896–5908. Fujita, M.; Tominaga, M.; Hori, A.; Therrien, B. *Acc. Chem. Res.* **2005**, *38*, 369–378. Leininger, S.; Olenyuk, B.; Stang, P. J. *Chem. Rev.* **2000**, *100*, 853–907.

(18) Very recently MacLachlan and co-workers have reported an elegant Pt-based MSPM system, see: Frischmann, P. D.; Guieu, S.; Tabeshi, R.; MacLachlan, M. J. *J. Am. Chem. Soc.* **2010**, *132*, 7668–7675.

(19) Lahiri, S.; Thompson, J. L.; Moore, J. S. *J. Am. Chem. Soc.* **2000**, *122*, 11315–11319. Moore, J. S.; Zhang, J. *Angew. Chem., Int. Ed. Engl.* **1992**, *31*, 922–924. Shetty, A. S.; Zhang, J.; Moore, J. S. *J. Am. Chem. Soc.* **1996**, *118*, 1019–1027. Zhang, J.; Moore, J. S. *J. Am. Chem. Soc.* **1992**, *114*, 9701–9702. Zhang, J.; Moore, J. S. *J. Am. Chem. Soc.* **1994**, *116*, 2655–2656. Zhang, J.; Pesak, D. J.; Ludwick, J. L.; Moore, J. S. *J. Am. Chem. Soc.* **1994**, *116*, 4227–4239. Zhao, D.; Moore, J. S. *J. Org. Chem.* **2002**, *67*, 3548–3554.

(20) Gower, M. L.; Crowley, J. D. *Dalton Trans.* **2010**, *39*, 2371–2378. Crowley, J. D.; Gavey, E. L. *Dalton Trans.* **2010**, *39*, 4035–4037. Crowley, J. D.; Bandeen, P. H. *Dalton Trans.* **2010**, *39*, 612–623. Crowley, J. D.; Steele, I. M.; Bosnich, B. *Eur. J. Inorg. Chem.* **2005**, 3907–3917. Crowley, J. D.; Goshe, A. J.; Bosnich, B. *Chem. Commun.* **2003**, 2824–2825.

(21) Crowley, J. D.; Steele, I. M.; Bosnich, B. *Inorg. Chem.* **2005**, *44*, 2989–2991. Crowley, J. D.; Bosnich, B. *Eur. J. Inorg. Chem.* **2005**, 2015–2025. Crowley, J. D.; Goshe, A. J.; Steele, I. M.; Bosnich, B. *Chem.—Eur. J.* **2004**, *10*, 1944–1955. Crowley, J. D.; Goshe, A. J.; Bosnich, B. *Chem. Commun.* **2003**, 392–393.

(22) While Ag(I) ions can adopt a variety of coordination numbers ranging from 2 to 6, complexes with pyridine donor ligands most commonly adopt a linear two-coordinate geometry. This $[Ag(Py)_2]^+$ motif has been used to form a variety of supramolecular structures including coordination polymers and metallo-macrocycles, see: Sumby, C. J.; Gordon, K. C.; Walsh, T. J.; Hardie, M. J. *Chem.—Eur. J.* **2008**, *14*, 4415–4425. Ronson, T. K.; Hardie, M. J. *CrystEngComm* **2008**, *10*, 1731–1734. Carruthers, C.; Ronson, T. K.; Sumby, C. J.; Westcott, A.; Harding, L. P.; Prior, T. J.; Riskallah, P.; Hardie, M. J. *Chem.—Eur. J.* **2008**, *14*, 10286–10296. Cunha-Silva, L.; Ahmad, R.; Carr, M. J.; Franken, A.; Kennedy, J. D.; Hardie, M. J. *Cryst. Growth Des.* **2007**, *7*, 658–667. Sumby, C. J.; Fisher, J.; Prior, T. J.; Hardie, M. J. *Chem.—Eur. J.* **2006**, *12*, 2945–2959. Sumby, C. J.; Carr, M. J.; Franken, A.; Kennedy, J. D.; Kilner, C. A.; Hardie, M. J. *New J. Chem.* **2006**, *30*, 1390–1396. Cunha-Silva, L.; Ahmad, R.; Hardie, M. J. *Aust. J. Chem.* **2006**, *59*, 40–48. Sumby, C. J.; Hardie, M. J. *Cryst. Growth Des.* **2005**, *5*, 1321–1324. Sumby, C. J.; Hardie, M. J. *Angew. Chem., Int. Ed.* **2005**, *44*, 6395–6399. Westcott, A.; Whitford, N.; Hardie, M. J. *Inorg. Chem.* **2004**, *43*, 3663–3672. Hardie, M. J.; Sumby, C. J. *Inorg. Chem.* **2004**, *43*, 6872–6874. Ahmad, R.; Hardie, M. J. *Cryst.Growth Des.* **2003**, *3*, 493–499. Steel, P. J.; Fitchett, C. M. *Coord. Chem. Rev.* **2008**, *252*, 990–1006. O'Keefe, B. J.; Steel, P. J. *CrystEngComm* **2007**, *9*, 222–227. Richardson, C.; Steel, P. J. *Eur. J. Inorg. Chem.* **2003**, 405–408. Steel, P. J.; Sumby, C. J. *Chem. Commun.* **2002**, 322–323. McMorran, D. A.; Steel, P. J. *Supramol. Chem.* **2002**, *14*, 79–85. McMorran, D. A.; Steel, P. J. *J. Chem. Soc., Dalton Trans.* **2002**, 3321–3326. McMorran, D. A.; Steel, P. J. *Inorg. Chem. Commun.* **1999**, *2*, 368–370. Richardson, C.; Steel, P. J. *Inorg. Chem. Commun.* **1998**, *1*, 260–262. O'Keefe, B. J.; Steel, P. J. *Inorg. Chem. Commun.* **1998**, *1*, 147–149. Hartshorn, C. M.; Steel, P. J. *J. Chem. Soc., Dalton Trans.* **1998**, 3927–3934. Hartshorn, C. M.; Steel, P. J. *J. Chem. Soc., Dalton Trans.* **1998**, 3935–3940. Hartshorn, C. M.; Steel, P. J. *Inorg. Chem.* **1996**, *35*, 6902–6903. Caradoc-Davies, P. L.; Hanton, L. R.; Henderson, W. *J. Chem. Soc., Dalton Trans.* **2001**, 2749–2755. Schultheiss, N.; Ellsworth, J. M.; Bosch, E.; Barnes, C. L. *J. Coord. Chem.* **2008**, *61*, 322–327. Bosch, E.; Barnes, C. L.; Brennan, N. L.; Eakins, G. L.; Breyfogle, B. E. *J. Org. Chem.* **2008**, *73*, 3931–3934. Bosch, E.; Barnes, C. L. *J. Coord. Chem.* **2005**, *58*, 1021–1027. Schultheiss, N.; Barnes, C. L.; Bosch, E. *Cryst. Growth Des.* **2003**, *3*, 573–580. Bosch, E.; Cordes, W. *J. Chem. Crystallogr.* **2003**, *33*, 723–726. Bosch, E.; Barnes, C. L. *Inorg. Chem.* **2001**, *40*, 3234–3236. Bosch, E.; Barnes, C. L. *Inorg. Chem.* **2001**, *40*, 3097–3100.

(23) It is well established that gold(I) prefers to form linear two-coordinate complexes. Recently Lin and co-workers have illustrated that $[Au(Py)_2]^+$ complexes can be synthesized, see: Lin, J. C. Y.; Tang, S. S.; Vasam, C. S.; You, W. C.; Ho, T. W.; Huang, C. H.; Sun, B. J.; Huang, C. Y.; Lee, C. S.; Hwang, W. S.; Chang, A. H. H.; Lin, I. J. B. *Inorg. Chem.* **2008**, *47*, 2543–2551.

Scheme 1. Synthesis of Silver(I)- or Gold(I)-Containing Planar MSPMs, **1** and **2**

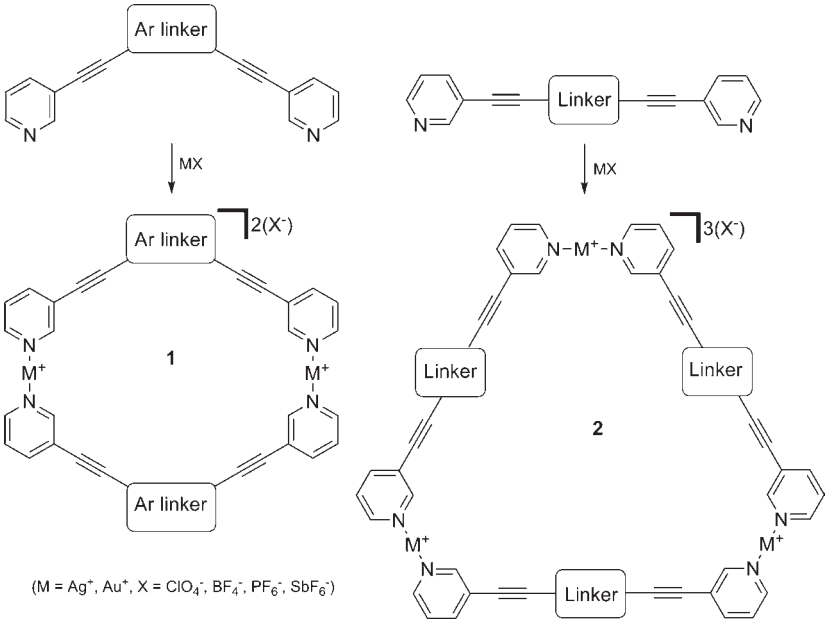

ligands[24] is expected to lead to the formation of the metallo-macrocycles, **1** and **2**, in high yield under thermodynamic control (Scheme 1). The use of ethynyl spacer units within the framework removes any steric interactions between the aromatic moieties of the ligands and allows for the formation of essentially perfectly planar macrocycles (Supporting Information, Figures S1−S2). Furthermore, the presence of the d^{10} metal ions within the macrocyclic framework is expected to be crucial for the generation of the well-defined metal−organic nanotube supra-structures. Because of the electrostatic nature of $\pi-\pi$ interactions,[25] planar aromatic molecules tend to form T-shaped or slipped stacked structures in the solid state and are therefore unsuitable, in isolation, for linear nanotube construction. On the other hand, it is well-established that many sterically unencumbered or planar d^{10} metal complexes stack in the crystalline state forming "weak" metal−metal interactions, which have strengths comparable to hydrogen bonds. Guided by the presence of the metal−metal interactions, this combination of supramolecular forces should lead to the formation of well-defined linear extended porous stacks (Supporting Information, Figures S1−S2). These planar MSPMs could potentially be useful building blocks for the synthesis of novel nanoscale materials.

Results and Discussion

Ligand Synthesis and Characterization. The bis(pyridylethynyl) ligands $\mathbf{L_2}$, $\mathbf{L_3}$, $\mathbf{L_4}$, and $\mathbf{L_5}$ were synthesized in good yields by a standard Pd/Cu catalyzed Sonogashira coupling reaction[26] between the appropriate dialkyne and 3-iodopyridine[27] (Scheme 2). Under these conditions, the yields of the ligands $\mathbf{L_2}$[28] and $\mathbf{L_3}$[29] are greatly increased from those that had been previously reported in the literature. As described previously, $\mathbf{L_1}$ was synthesized via a Glaser homocoupling of 3-ethynylpyridine.[30] To the best of our knowledge this is the first report on the synthesis of both $\mathbf{L_4}$ and $\mathbf{L_5}$ and as such both ligands have been fully characterized by IR and NMR spectroscopy (Supporting Information, Figures S3−S7), ESI-MS, and elemental analysis.

Silver(I) and Gold(I) Complexes. The silver(I) complexes of the ligands $\mathbf{L_1}-\mathbf{L_5}$ were prepared by the addition of a molar equivalent of silver salt (AgX, X = BF_4^-, SbF_6^-, $SO_3CF_3^-$, or ClO_4^-) to an acetone solution of the ligand. The complexes precipitated immediately from the solution in good to excellent yields (49−97%) as analytically pure white solids, which appear moderately stable both in the solid state and in solution when stored in the

(24) Bis(pyridylethynyl) ligands have previously been shown to form coordination polymers and metallo-macrocycles with a variety of metal ions, see: Liao, P.; Langloss, B. W.; Johnson, A. M.; Knudsen, E. R.; Tham, F. S.; Julian, R. R.; Hooley, R. J. *Chem. Commun.* **2010**, *46*, 4932–4934. Zhao, G.-J.; Northrop, B. H.; Stang, P. J.; Han, K.-L. *J. Phys. Chem. A* **2010**, *114*, 3418–3422. Ghosh, S.; Gole, B.; Bar, A. K.; Mukherjee, P. S. *Organometallics* **2009**, *28*, 4288–4296. Kim, H.-J.; Lee, E.; Kim, M. G.; Kim, M.-C.; Lee, M.; Sim, E. *Chem.—Eur. J.* **2008**, *14*, 3883–3888. Kim, H.-J.; Lee, J.-H.; Lee, M. *Angew. Chem., Int. Ed.* **2005**, *44*, 5810–5814. Kim, H.-J.; Zin, W.-C.; Lee, M. *J. Am. Chem. Soc.* **2004**, *126*, 7009–7014. Chi, K.-W.; Addicott, C.; Arif, A. M.; Das, N.; Stang, P. J. *J. Org. Chem.* **2003**, *68*, 9798–9801. Chi, K.-W.; Addicott, C.; Kryschenko, Y. K.; Stang, P. J. *J. Org. Chem.* **2004**, *69*, 964–966. Akhtaruzzaman, M.; Tomura, M.; Zaman, M. B.; Nishida, J.-i.; Yamashita, Y. *J. Org. Chem.* **2002**, *67*, 7813–7818. Zaman, M. B.; Smith, M. D.; Ciurtin, D. M.; Zur Loye, H.-C. *Inorg. Chem.* **2002**, *41*, 4895–4903. Zaman, M. B.; Udachin, K.; Akhtaruzzaman, M.; Yamashita, Y.; Ripmeester, J. A. *Chem. Commun.* **2002**, 2322–2323. Zaman, M. B.; Udachin, K.; Ripmeester, J. A.; Smith, M. D.; Zur Loye, H.-C. *Inorg. Chem.* **2005**, *44*, 5047–5059. Zaman, M. B.; Udachin, K. A.; Ripmeester, J. A. *CrystEngComm* **2002**, *4*, 613–617.

(25) Hunter, C. A.; Lawson, K. R.; Perkins, J.; Urch, C. J. *J. Chem. Soc., Perkin Trans. 2* **2001**, 651–669. Meyer, E. A.; Castellano, R. K.; Diederich, F. *Angew. Chem., Int. Ed.* **2003**, *42*, 1210–1250.

(26) Sonogashira, K. *J. Organomet. Chem.* **2002**, *653*, 46–49. Sonogashira, K.; Tohda, Y.; Hagihara, N. *Tetrahedron Lett.* **1975**, 4467–4470. Chinchilla, R.; Najera, C. *Chem. Rev.* **2007**, *107*, 874–922.

(27) Krasnokutskaya, E. A.; Semenischeva, N. I.; Filimonov, V. D.; Knochel, P. *Synthesis* **2007**, 81–84.

(28) Grummt, U. W.; Birckner, E.; Klemm, E.; Egbe, D. A. M.; Heise, B. *J. Phys. Org. Chem.* **2000**, *13*, 112–126.

(29) Schultheiss, N.; Ellsworth, J. M.; Bosch, E.; Barnes, C. L. *Eur. J. Inorg. Chem.* **2005**, 45–46.

(30) Rodriguez, J. G.; Martin-Villamil, R.; Cano, F. H.; Fonseca, I. *J. Chem. Soc., Perkin Trans. 1* **1997**, 709–714.

Scheme 2. Synthesis of Bis(pyridylethynyl) Ligands Used in This Study[a]

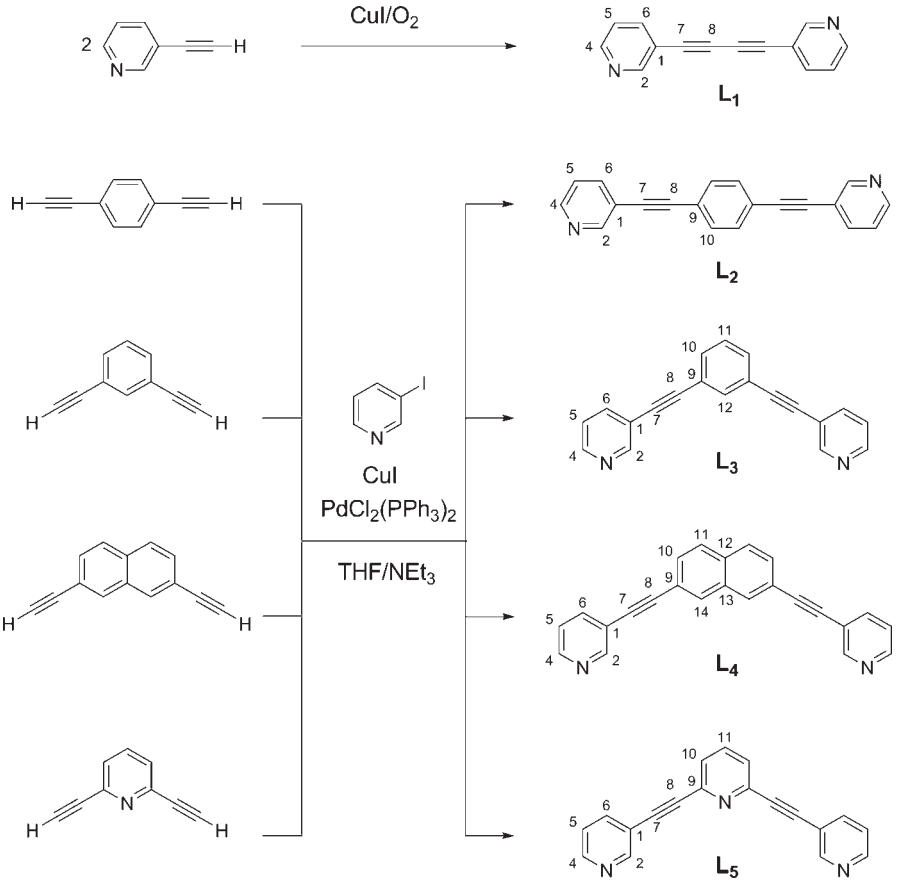

[a] Isolated yields, $\mathbf{L_1}$ (88%), $\mathbf{L_2}$ (65%), $\mathbf{L_3}$ (90%), $\mathbf{L_4}$ (76%), $\mathbf{L_5}$ (81%).

absence of light. The complexes are slightly soluble in acetone, but demonstrate much better solubility in more coordinating solvents such as acetonitrile and dimethylsulfoxide.

Following on from the successful synthesis and isolation of the Ag(I) complexes we attempted to extend this chemistry to Au(I). Following a recently published synthetic route to cationic bispyridyl Au(I) complexes,[23] ligands $\mathbf{L_1}$ or $\mathbf{L_3}$ were reacted with a molar equivalent of $AuCl(SMe)_2$ and NH_4PF_6 in dichloromethane/ethanol. During the course of the reaction a noticeable amount of purple solid formed, which we suspect to be Au(0) nanoparticles, and no pure product could be isolated. Alternatively, transmetallation from the Ag(I) complexes with $AuCl(SMe_2)$ in acetonitrile was also attempted. However, after filtration to remove AgCl the solution slowly became purple. Nevertheless, a white solid was obtained from the reaction mixture, and although microanalysis of several different preparations was nonreproducible, high resolution electrospray ionization mass spectrometry (HR-ESI-MS) indicated that the gold(I) macrocycles are formed in solution (Supporting Information, Figures S8−S9). However, the cationic gold(I) macrocyclic complexes were only soluble in coordinating solvents, and disappointingly, over a 2 h period, solutions of the Au(I) macrocycles changed from colorless to purple indicating that the complexes had decomposed into gold nanoparticles (AuNP).[31] Because of the instability of these Au(I) complexes, they were not pursued further.

Spectrometric and Spectroscopic Characterization of Silver Complexes. Microelemental analyses of the Ag(I) complexes were consistent with a 1:1:1 ligand/silver/anion ratio. FT-IR data of the isolated Ag(I) complexes revealed the alkyne stretching wave number to range from 2232 to 2220 cm^{-1}; the values are slightly increased from those observed in the free ligands (2221−2206 cm^{-1}) and are indicative of transfer of electron density from the alkyne moiety of the ligand to the Ag(I) cations.

A comparison between ^1H and ^{13}C NMR spectra of the ligands and the Ag(I) complexes in d_3-acetonitrile (in which all complexes are moderately soluble) shows only minute changes in proton environments (Supporting Information, Figures S10−S12), presumably because the coordinating solvent establishes an equilibrium between the free ligand and the Ag(I) salt. Fortunately, the complexes containing SbF_6^- anions were slightly soluble in d_6-acetone, and ^1H NMR spectra were able to be acquired.

(31) Similar decomposition of Au(I)−Py complexes, in coordinating solvents, has been observed see: Chiou, J. Y. Z.; Luo, S. C.; You, W. C.; Bhattacharyya, A.; Vasam, C. S.; Huang, C. H.; Lin, I. J. B. *Eur. J. Inorg. Chem.* **2009**, 1950–1959. While it is unclear what the reducing agent is, presumably the coordinating solvents cause dissociation of the pyridine ligands from the gold(I) ions which allows the Au atoms to aggregate into AuNP. It is well established that pyridine ligands can stabilize AuNP, see;. Ghosh, S. K. *Colloids Surf., A* **2010**, *371*, 98–103. Gandubert, V. J.; Lennox, R. B. *Langmuir* **2005**, *21*, 6532–6539. Rucareanu, S.; Gandubert, V. J.; Lennox, R. B. *Chem. Mater.* **2006**, *18*, 4674–4680.

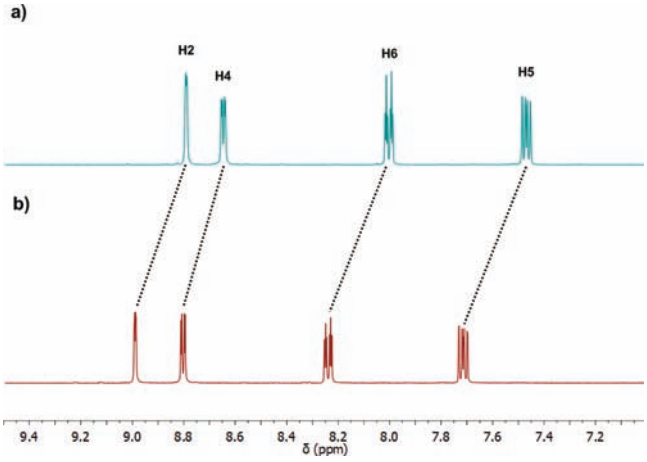

Figure 1. Stacked ^{1}H NMR spectra (298 K, 2 mM) of (a) $\mathbf{L_1}$ and (b) $\{[\mathbf{L_1}Ag](SbF_6)\}_n$ in d_6-acetone.

A comparison of the ^{1}H NMR data of $\mathbf{L_1}$ and $\{[\mathbf{L_1}Ag](SbF_6)\}_n$ is shown in Figure 1. Considerable downfield shifts for all proton signals were observed indicating the Ag(I) ions are strongly coordinated to $\mathbf{L_1}$. Comparable shifts are also observed for the SbF_6^- containing complexes of $\mathbf{L_2}-\mathbf{L_5}$.

The nature of the species present in solution was probed further by examining CH_3CN solutions of the silver complexes by positive ion HR-ESI-MS. The identity of every ion was verified by comparison of the isotopic patterns of the observed peak with the theoretical simulation (for examples see Supporting Information, Figures S13−S18). The ESI-MS spectra of the silver(I) complexes **1** ($\mathbf{L_3}$, $\mathbf{L_4}$, $\mathbf{L_5}$) were dominated by peaks corresponding to $[Ag_2(L)_2](X)^+$ along with the monomeric $[Ag(L)_2]^+$ or $[AgL]^+$ fragment ions indicating that the dimeric metallocyclic structures are present in solution. Additionally, in the case of **1** ($\mathbf{L_3}$, $\mathbf{L_4}$, X = ClO_4^-, BF_4^-) overlapping but isotopically resolved peaks due to $[Ag_2(L)_2]^{2+}$ and $[AgL]^+$, provided further support for the postulate that the metallomacrocycles are formed in solution and the gas phase (Supporting Information, Figures S13−S18). Similarly, the silver(I) complexes **2** ($\mathbf{L_1}$, $\mathbf{L_2}$) show ions due to the trimeric $[Ag_3(L)_3](2X)^+$ species in addition to the smaller dimeric $[Ag_2(L)_2](X)^+$ and $[Ag_2(L)_2]^{2+}$ species and the monomeric $[Ag(L)_2]^+$ or $[AgL]^+$ fragment ions. Although in combination the ^{1}H NMR and ESI-MS data are consistent with the presence of metallo-macrocycles in solution, they do not rule out the possibility that the observed silver complexes are oligomers.[32] However, it is well established that discrete metallo-macrocycles are enthalpically more stable than the corresponding oligomers, supporting the idea that the observed species are in fact the desired discrete metallo-macrocycles.[17] The presence of ions due to $[Ag_3(L)_3](2X)^+$ and $[Ag_2(L)_2](X)^+$ in the ESI-MS spectra of **2** ($\mathbf{L_1}$, $\mathbf{L_2}$), suggests that both 2:2 and 3:3 metallo-macrocycles (Supporting Information, Figure S19) are formed in solution, and this is presumably due to the subtle thermodynamic balance between enthalpic and entropic factors as has been observed previously in related systems.[33] To conclusively prove the formation of metallo-macrocycles and examine if they would self-assemble into metal−organic nanotubes, we undertook an X-ray crystallographic study of the complexes. Fortunately we were able to obtain X-ray quality crystals of the complexes **1** ($\mathbf{L_3}$ and $\mathbf{L_5}$, X = ClO_4^-) along with the $AgSbF_6$ and $AgClO_4$ complexes of $\mathbf{L_1}$.

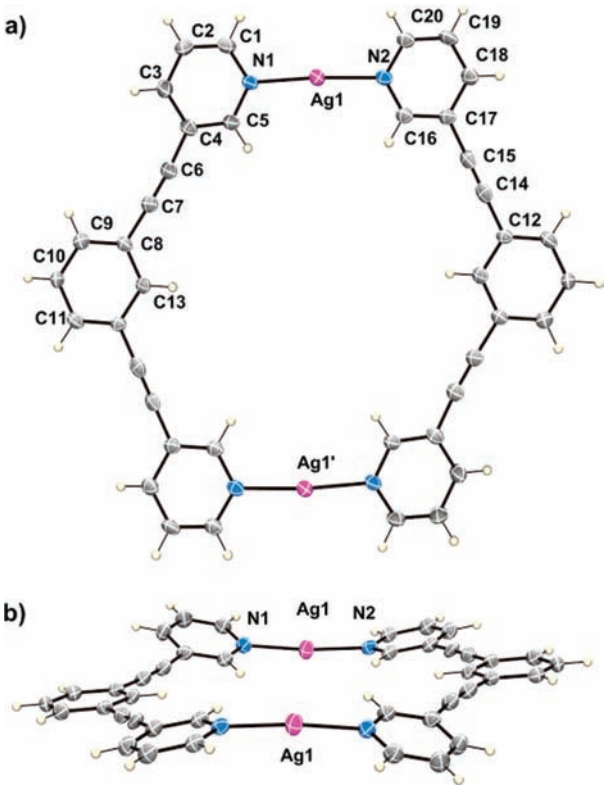

Figure 2. Labeled ORTEP diagrams of MSPM **1** ($\mathbf{L_3}$, X = ClO_4^-); (a) a top view, (b) a side view. The thermal ellipsoids are shown at the 50% probability level. The ClO_4^- anions and disordered water molecules have been omitted for clarity. Selected bond lengths (Å) and angles (deg); Ag1−N1 2.145(4), Ag1−N2 2.146(4), N1−Ag1−N2 171.3(1). Symmetry code; $2-x$, $1-y$, $1-z$.

X-ray Crystallographic Characterization. X-ray quality crystals of **1** ($\mathbf{L_3}$, X = ClO_4^-) were obtained by vapor diffusion of diethyl ether into an acetonitrile solution of the complex. The molecule crystallizes in the triclinic space group $P\bar{1}$ as the expected 2:2 metallo-macrocycle, $[(\mathbf{L_3})_2Ag_2](ClO_4)_2$, with two molecules in the unit cell (Figure 2a). The N1−Ag1 and N2−Ag1 bond distances are 2.145(4) Å and 2.146(4) Å, respectively, and these are typical lengths of a pyridyl-Ag(I) bond. The N1−Ag1−N2

(32) For related silver(I) metallo-macrocycles that have been characterized in solution using ^{1}H NMR and ESI-MS see: Wei, W.; Wu, M.; Huang, Y.; Gao, Q.; Zhang, Q.; Jiang, F.; Hong, M. *CrystEngComm* **2009**, *11*, 576–579. Chen, C.-L.; Yu, Z.-Q.; Zhang, Q.; Pan, M.; Zhang, J.-Y.; Zhao, C.-Y.; Su, C.-Y. *Cryst. Growth Des.* **2008**, *8*, 897–905. Yue, N. L. S.; Jennings, M. C.; Puddephatt, R. J. *Eur. J. Inorg. Chem.* **2007**, 1690–1697. Aly, A. A. M.; Vatsadze, S. Z.; Chernikov, A. V.; Walfort, B.; Rueffer, T.; Lang, H. *Polyhedron* **2007**, *26*, 3925–3929. Chen, C.-L.; Tan, H.-Y.; Yao, J.-H.; Wan, Y.-Q.; Su, C.-Y. *Inorg. Chem.* **2005**, *44*, 8510–8520. Caradoc-Davies, P. L.; Hanton, L. R. *Dalton Trans.* **2003**, 1754–1758.

(33) Ghosh, S.; Mukherjee, P. S. *Inorg. Chem.* **2009**, *48*, 2605–2613. Weilandt, T.; Troff, R. W.; Saxell, H.; Rissanen, K.; Schalley, C. A. *Inorg. Chem.* **2008**, *47*, 7588–7598. Ferrer, M.; Gutierrez, A.; Mounir, M.; Rossell, O.; Ruiz, E.; Rang, A.; Engeser, M. *Inorg. Chem.* **2007**, *46*, 3395–3406. Cotton, F. A.; Murillo, C. A.; Yu, R. *Dalton Trans.* **2006**, 3900–3905. Ferrer, M.; Mounir, M.; Rossell, O.; Ruiz, E.; Maestro, M. A. *Inorg. Chem.* **2003**, *42*, 5890–5899. Sautter, A.; Schmid, D. G.; Jung, G.; Wuerthner, F. *J. Am. Chem. Soc.* **2001**, *123*, 5424–5430. Fujita, M.; Sasaki, O.; Mitsuhashi, T.; Fujita, T.; Yazaki, J.; Yamaguchi, K.; Ogura, K. *Chem. Commun.* **1996**, 1535–1536.

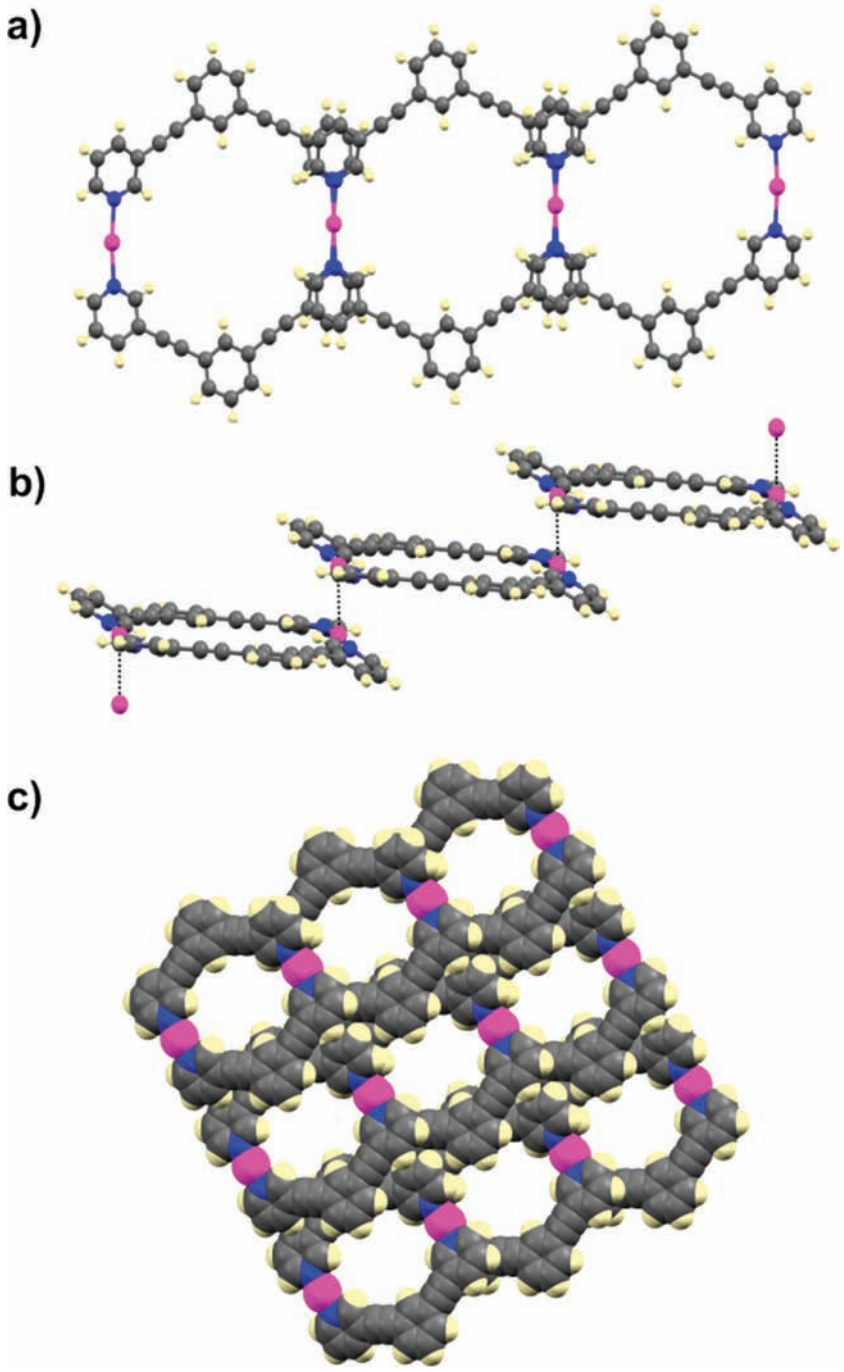

Figure 3. Ball-and-stick and space-filling representations of the MSPM **1** ($\mathbf{L_3}$, X = ClO_4^-). (a) A top view (ball-and-stick representation) of the step polymer structure, (b) a side view (ball-and-stick representation) of the step polymer structure, (c) a space filling representation showing the pores within the structure. The ClO_4^- anions and disordered water molecules that fill the pores have been omitted for clarity. The Ag(I)---Ag(I) distance in the step polymer chains is 3.146(1) Å. Color scheme: Gray = carbon, blue = nitrogen, pink = silver.

angle is 171.3(1)°, and this is consistent with the preference of Ag(I) to adopt a linear two-coordinate coordination geometry with pyridyl donor ligands. The small deviation of this angle from 180° is due to close contact of the ClO_4^- counterion to the Ag(I) cations (Supporting Information, Figures S20−S22, Ag−O bond distances for Ag1−O1 and Ag1′−O2 are 2.861(5) Å and 2.795(4) Å). Although the central phenyl ring and the N1-containing pyridyl group are essentially coplanar, the N2-containing pyridyl unit is twisted by 23° out of the plane making the macrocyclic framework slightly non-planar (Figure 2b).

Disappointingly, despite the planarity of the MSPM, **1** ($\mathbf{L_3}$, X = ClO_4^-), the desired linear metal−organic nanotubes were not formed in the extended crystal structure. Instead, a step-polymer of macrocycles, stabilized by a combination of π-stacking (centroid−centroid distance 3.902 Å) and metal−metal interactions (Ag---Ag distance 3.146(1) Å) was obtained (Figures 3a and b). π-Stacking interactions (centroid−centroid distance 3.829 Å) between the neighboring step-polymer strands result in the formation of a nanoporous chicken-wire structure (Figure 3c). The nanoporous channels within the structure

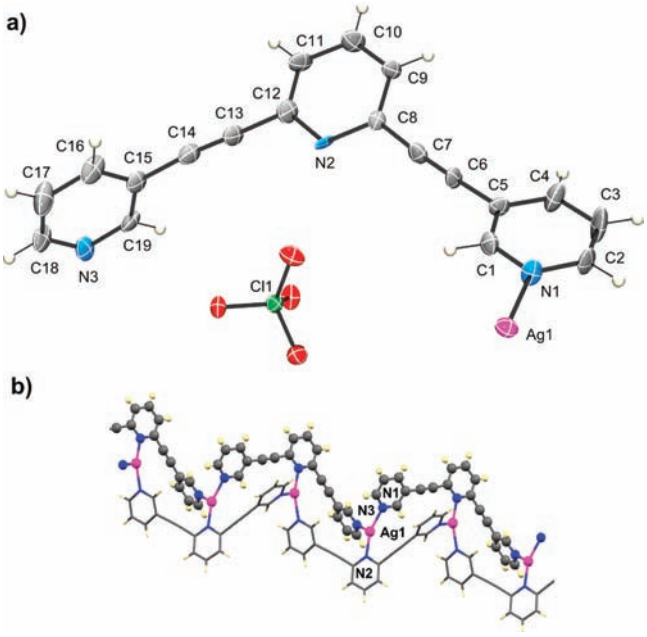

Figure 4. (a) Labeled ORTEP diagram of the asymmetric unit of $\{[\mathbf{L_5}Ag](ClO_4)\cdot 0.5Et_2O\}_n$. The thermal ellipsoids are shown at the 50% probability level. The disordered diethyl ether solvate has been omitted for clarity. (b) A ball-and-stick and tube representation of the ladder polymer structure formed by $\{[\mathbf{L_5}Ag](ClO_4)\cdot 0.5Et_2O\}_n$. The ClO_4^- anions and solvent molecules have been omitted for clarity. Selected bond lengths (Å) and angles (deg); Ag1−N1 2.261(8), Ag1−N2 2.23(1), Ag1−N3 2.32(1), N1−Ag1−N2 138.7(4), N1−Ag1−N3 102.2(4), N2−Ag1−N3 119.0(4). Symmetry code; x, $1 + y$, z. Color scheme: Gray = carbon, blue = nitrogen, cream = hydrogen, and pink = silver.

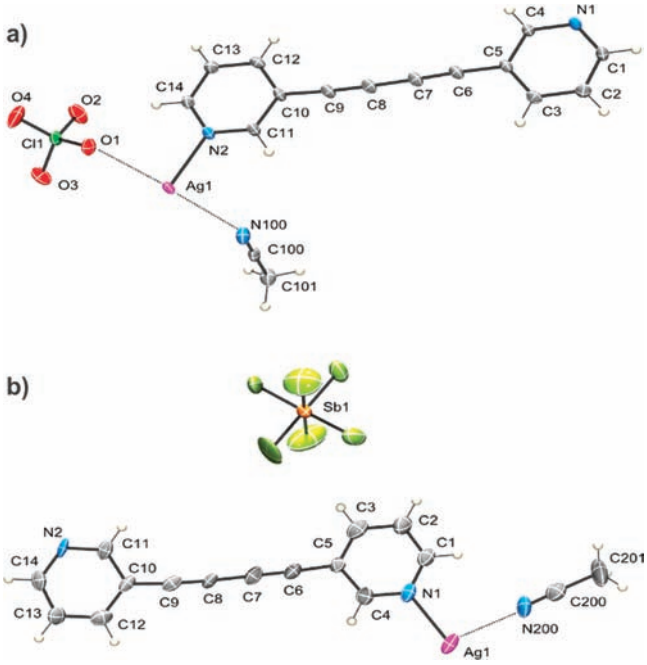

Figure 5. Labeled ORTEP diagrams of asymmetric units for $\{[\mathbf{L_1}Ag(CH_3CN)](ClO_4)\}_n$ (a) and $\{[\mathbf{L_1}Ag(CH_3CN)](SbF_6)\cdot CH_3CN\}_n$ (b) coordination polymers. The thermal ellipsoids are shown at the 50% probability level. Non-coordinated solvates have been omitted for clarity.

are filled with ClO_4^- and disordered H_2O molecules (Supporting Information, Figures S20−S22).[34]

In an effort to alter the packing arrangement and generate the desired linear metal−organic nanotubes we examined the crystallization of **1** ($\mathbf{L_4}$ and $\mathbf{L_5}$; X = BF_4^-, SbF_6^-, $SO_3CF_3^-$, or ClO_4^-). Repeated attempts to crystallize **1** ($\mathbf{L_4}$; X = BF_4^-, SbF_6^-, $SO_3CF_3^-$, or ClO_4^-) only resulted in the rapid precipitation and isolation of amorphous colorless solids, presumably because of the modest solubility of these complexes in all solvents.

Vapor diffusion of diethyl ether into an acetonitrile solution of **1** ($\mathbf{L_5}$ X = ClO_4^-) provided X-ray quality crystals of the complex. However, despite the solution data being consistent with the formation of the 2:2 metallo-macrocycle, in the solid state the macrocycle ring opens and crystallizes as a coordination polymer. The perchlorate complex of $\mathbf{L_5}$ crystallizes in the monoclinic space group $P2_1/n$ with the asymmetric unit consisting of one ligand, one silver cation, a perchlorate anion, and half a molecule of disordered diethyl ether. The central pyridyl nitrogen, which was incorporated into $\mathbf{L_5}$ in an attempt to enhance the face-to-face π-stacking interactions between the macrocycles, is found to coordinate to the Ag(I) ions generating a twisted ladder polymer (Figure 4). The Ag(I) ion adopts an approximately trigonal-planar geometry (Ag−N bond-angle range: 102.2 to 138.7°). Because of steric congestion, the Ag−N bond distances (2.23(1), 2.261(8), and 2.32(1) Å) are somewhat longer than those observed in the other structures. The perchlorate anion sits in a pocket bridging two Ag(I) cations of the polymer chain (Ag1−O2 2.824(9) and Ag1′−O4 3.446(8) Å; see Supporting Information, Figure S23). Individual polymer strands are closely packed together, and this interaction is stabilized by a face-to-face π-stacking interaction (centroid−centroid distance 3.645 Å) between the ligands central pyridyl ring on adjacent polymers.

Similar ring-opening behavior is observed for the trisilver(I) macrocycles, **2** ($\mathbf{L_1}$ X = ClO_4^- and SbF_6^-). X-ray quality crystals of the $\mathbf{L_1}$AgX (X = ClO_4^- and SbF_6^-) complexes were obtained by the slow diffusion of diethyl ether into acetonitrile solutions of the silver complexes at room temperature. The perchlorate complex of $\mathbf{L_1}$ crystallizes in the *Pbca* space group with the asymmetric unit consisting of one ligand, one silver cation, a perchlorate anion, and an acetonitrile molecule. In the solid state, the structure of $\mathbf{L_1}$AgX is not the desired macrocycle, **2** ($\mathbf{L_1}$, X = ClO_4^-) but an infinite coordination polymer, a portion of which is shown in Figures 5 and 6. Each silver cation has pseudo square-planar geometry; in addition to being coordinated to two ligands (the Ag−N bond distances, 2.199(2) and 2.202(1) Å), there are also weak silver−oxygen (Ag−O bond distance 2.675(1) Å) and silver−nitrogen (Ag−N bond distance 2.648(2) Å) interactions to perchlorate and acetonitrile molecules, respectively. The SbF_6^- complex of $\mathbf{L_1}$ has a similar structure with an infinite polymeric network running through the crystal (Figures 5 and 6). The change from a coordinating (ClO_4^-) to a non-coordinating (SbF_6^-) anion causes a change in the geometry around the silver center, which now adopts a three-coordinate T-shaped arrangement.

(34) We were also able to generate very small crystals from an acetonitrile solution of the $[(\mathbf{L_3})_2Ag_2](SbF_6)_2$ macrocycle. In this case the macrocycle had ring-opened and crystallized as a complicated disordered coordination polymer, indicating that the counteranion plays an important role in the formation of the solid-state structure, see Supporting Information, Figures S24−S26.

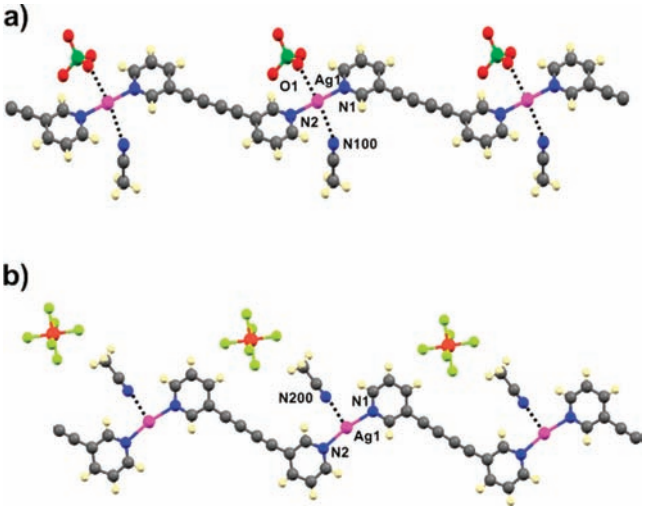

Figure 6. Ball-and-stick representations of the solid-state structures for the $\{[\mathbf{L_1}Ag(CH_3CN)](ClO_4)\}_n$ (a) and $\{[\mathbf{L_1}Ag(CH_3CN)](SbF_6)\cdot CH_3CN\}_n$ (b) coordination polymers. Selected bond lengths (Å) and angles (deg) for $\{[\mathbf{L_1}Ag](ClO_4)\}_n$: Ag1−N1 2.202(1), Ag1−N2 2.199(2), Ag1−N100 2.648(2), Ag1−O1 2.675(1), N1−Ag1−N2 179.41(1), N100−Ag1−O1 163.93(5). Symmetry code; $-1 + x$, y, z. Selected bond lengths (Å) and angles (deg) for $\{[\mathbf{L_1}Ag(CH_3CN)](SbF_6)\cdot CH_3CN\}_n$: Ag1−N1 2.159(7), Ag1−N2 2.167(8), Ag1−N200 2.59(1), N1−Ag1−N2 169.7(3), N200−Ag1−N1 95.6(3), N200−Ag1−N2 94.4(3). Symmetry code; $-1 + x$, $1 + y$, z. Color scheme: Gray = carbon, blue = nitrogen, red = oxygen, green = chlorine, yellow = fluorine, orange = antimony, and pink = silver.

The Ag(I) center is surrounded by two N-coordinated pyridyl donor ligands (Ag−N bond distances 2.159(7) and 2.167(8) Å) and an N-coordinated acetonitrile molecule (Ag−N bond distance 2.59(1) Å) and in addition a non-coordinating acetonitrile is also present.

In both $\mathbf{L_1}$ containing silver(I) complexes, the infinite polymeric chains stack upon each other (Figure 7). In the perchlorate example, π-stacking interactions are present between the pyridyl rings of the chain. In addition, O1 of a perchlorate anion acts as a weak bridge between the two chains. Conversely, the chains of the SbF_6^- example are stacked on top of each other exploiting Ag-π interactions. The silver in one chain interacts with the π-alkyne system of a chain above and the π-system of a pyridyl ring in the chain below. Somewhat surprisingly, no Ag---Ag interactions are present in either structure.

Although the ^{1}H NMR and ESI-MS data indicate that the desired planar metallo-macrocycles are present in solution only one, **1** ($\mathbf{L_3}$ X = ClO_4^-), persists in the solid state, and despite forming the desired planar MSPM it does not self-assemble into a linear cofacially stacked metal−organic nanotube. While the crystal structure of the planar macrocycle exhibits both π-stacking and metal−metal interactions a slip-stacked step-polymer is formed instead of the desired linearly stacked metal−organic nanotube. The natural tendency of aromatic π systems coupled with electrostatic repulsion between the cationic MSPM building blocks presumably leads to the

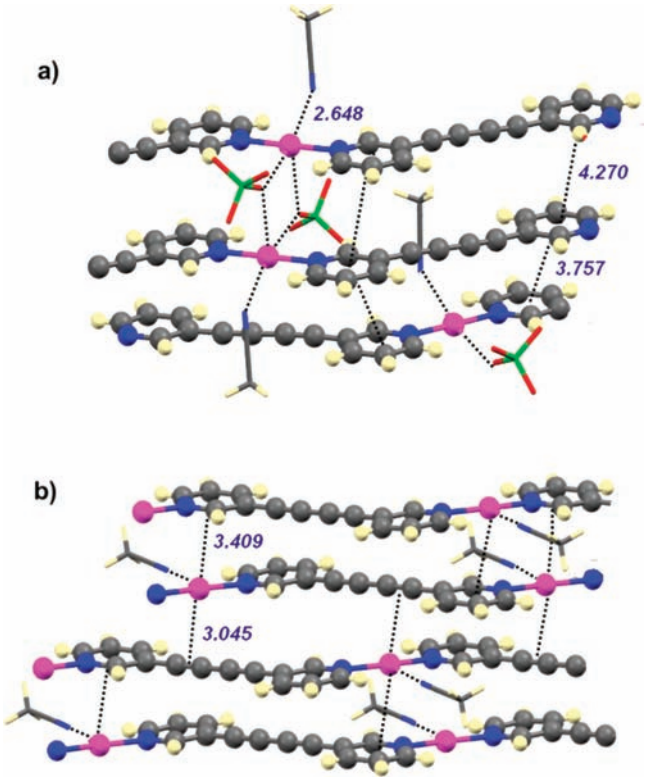

Figure 7. Ball-and-stick representations of the repeating packing interactions present between the infinite polymeric chains of (a) $\{[\mathbf{L_1}Ag](ClO_4)\cdot CH_3CN\}_n$ and (b) $\{[\mathbf{L_1}Ag(CH_3CN)](SbF_6)\cdot CH_3CN\}_n$. The SbF_6^- anions have been omitted for clarity. Color scheme: Gray = carbon, blue = nitrogen, red = oxygen, green = chlorine, and pink = silver.

formation of the slip-stacked structure.[35] Although the desired linear metal−organic nanotubes are not generated the structure still contains nanopores which are filled with disordered water molecules. X-ray crystallography of the silver(I) complexes of $\mathbf{L_1}$ and $\mathbf{L_5}$ show that the metallo-macrocycles have ring-opened and crystallize as non-porous coordination polymers.[36] The lability of the silver(I) ions enables the metallo-macrocycles to rearrange into the linear polymers during the crystallization process. We postulate that the rearrangement process is driven by crystal packing forces, the coordination polymers are able to form close-packed non-porous structures, whereas the silver(I) macrocycles would presumably form less efficiently packed porous materials. Although **1** and **2** were designed to form MSPMs, the resulting structures are not all shape-persistent presumably because of the lability of the silver(I)-pyridine interactions. These observations suggest that less labile metal ions such as Au(I)[37] and Pt(II),[18] which would not rearrange during attempted crystallizations, should be incorporated in the framework of the planar metallo-macrocycles to enable them to be used as building blocks for the self-assembly of linear metal−organic nanotubes.

(35) While it may seem obvious that electrostatic repulsion between the cationic macrocycles would prevent the desired stacking interactions, there are examples in the literature where cationic planar SPM are found to adopt a face-to-face stacked arrangement, see: Maekawa, M.; Kitagawa, S.; Kuroda-Sowa, T.; Munakata, M. *Chem. Commun.* **2006**, 2161–2163. Klyatskaya, S.; Dingenouts, N.; Rosenauer, C.; Mueller, B.; Hoeger, S. *J. Am. Chem. Soc.* **2006**, *128*, 3150–3151.

(36) For a recent experimental study on the ring opening of silver(I) metallo-macrocycles see: Yue, N. L. S.; Jennings, M. C.; Puddephatt, R. J. *Dalton Trans.* **2010**, *39*, 1273–1281.

(37) Kilpin, K. J.; Horvath, R.; Jameson, G. B.; Telfer, S. G.; Gordon, K. C.; Crowley, J. D. *Organometallics* **2010**, *29*, 6186–6195. Kilpin, K. J.; Paul, U. S. D.; Lee, A.-L.; Crowley, J. D. *Chem. Commun.* **2011**, DOI: 10.1039/C1030CC02185G

Experimental Section

General Experimental Section. NMR experiments were carried out on either a Varian 400-MR or a Varian 500 MHz VNMRS spectrometer operating at 298 K with chemical shifts referenced to residual solvent peaks ($CDCl_3$: ^1H δ 7.26 ppm, ^{13}C δ 77.16 ppm; CD_3CN: ^1H 1.94, ^{13}C 1.32, 118.26 ppm; d_6-acetone ^1H δ 2.05 ppm, ^{13}C δ 206.68 and 29.92 ppm). Chemical shifts are reported in parts per million (ppm) and coupling constants (J) in hertz (Hz). Standard abbreviations indicating multiplicity were used as follows: m = multiplet, t = triplet, d = doublet, s = singlet, b = broad. High resolution ESI-MS analysis was carried out using acetonitrile solutions on a Bruker MicrOTOF-Q spectrometer. IR spectroscopy was carried out using a Bruker ALPHA FT-IR spectrometer with an ALPHA P ATR measurement module. Melting points were determined on a Sanyo Gallenkamp apparatus and are uncorrected. Microelemental analysis was carried out at the Campbell Microanalytical Laboratory at the University of Otago. 3-Ethynylpyridine, 1,4-diethynylbenzene, 1,3-diethynylbenzene, $AgClO_4$, $AgSbF_6$, $AgBF_4$, and $AgSO_3CF_3$ were purchased from commercial sources and used as received. 3-Iodopyridine,[27] $\mathbf{L_1}$[30] 2,7-diethynylnaphthalene,[38] and 2,6-diethynylpyridine[39] were synthesized using literature procedures.

General Sonagashira Coupling Procedure[26] for the Preparation of L_2, L_3, L_4, and L_5. Under an argon atmosphere CuI (0.2 equiv) and $Pd(PPh_3)_2Cl_2$ (0.1 equiv), followed by the dialkyne (l equiv), were added to a previously degassed solution of 3-iodopyridine (2 equiv) in THF and triethylamine (1:1). The resulting yellow solution was stirred at room temperature (RT) for 18 h then diluted with ethylacetate (50 mL) and vigorously stirred with aqueous EDTA/NH_4OH (100 mL, 1M) for 1 h. The resulting organic phase was washed with saturated aqueous NH_4Cl (50 mL), water (50 mL), and brine (50 mL) and dried with anhydrous $MgSO_4$. The solvent was removed under vacuum to give a yellow solid which was further purified by column chromatography (SiO_2, CH_2Cl_2/acetone gradient 100:0 to 50:50) to give the ligand as a pale yellow solid.

1,4-Bis(pyridin-3-ylethynyl)benzene, L_2. CuI (0.09 g, 0.49 mmol), $Pd(PPh_3)_2Cl_2$ (0.17 g, 0.24 mmol), 1,4-diethynylbenzene (0.31 g, 2.44 mmol), and 3-iodopyridine (1.00 g, 4.88 mmol) in THF (20 mL) and triethylamine (20 mL) to yield $\mathbf{L_2}$ as a pale yellow solid (0.49 g, 65%). Mp: 182−183 °C; IR (ATR): $\bar{\nu}$ 2206, 1556, 1505, 1473, 1406, 1188, 1120, 1020, 847, 835, 815, 799, 699, 654, 623, 546, 520, 447 cm^{-1}; ^1H NMR (500 MHz, CD_3CN): δ 8.76 (d, J = 1.5 Hz, 2H, H-2), 8.57 (dd, J = 4.8, 1.5 Hz, 2H, H-4), 7.90 (dt, J = 7.9, 1.9 Hz, 2H, H-6), 7.61 (s, 4H, H-10), 7.39 (ddd, J = 4.8, 7.9, 0.6 Hz, 2H, H-5); ^{13}C (125 MHz): δ 153.1 (C-2), 150.2 (C-4), 139.5 (C-6), 132.9 (C-10), 124.5 (C-5), 124.0 (C-9), 120.9 (C-1), 92.5 (C-8), 89.1 (C-7) ppm; HR-ESI MS (DCM/MeOH): m/z 281.107 ($[\mathbf{L_2}+H]^+$, calcd for $C_{20}H_{13}N_2$ 281.107), 303.089 ($[\mathbf{L_2}+Na]^+$, calcd for $C_{20}H_{12}N_2Na$ 303.089); Anal. Calcd for $C_{20}H_{12}N_2$: C 85.69, H 4.31, N 9.99. Found: C 85.61, H 4.21, N 9.69%

1,3-Bis(pyridin-3-ylethynyl)benzene, L_3. CuI (0.120 g, 0.63 mmol), $Pd(PPh_3)_2Cl_2$ (0.105 g, 0.15 mmol), 1,3-diethynylbenzene (0.398 g, 3.15 mmol), and 3-iodopyridine (1.29 g, 6.30 mmol) in THF (20 mL) and triethylamine (20 mL) to yield $\mathbf{L_3}$ as a pale yellow solid (0.807 g, 90%). Mp: 61−63 °C; IR (ATR): $\bar{\nu}$ 2211, 1594, 1574, 1557, 1480, 1409, 1186, 1096, 1020, 908, 808, 794, 701, 682, 539, 526, 469, 433 cm^{-1}; ^1H NMR (500 MHz, CD_3CN): δ 8.76 (d, J = 1.6 Hz, 2H, H-2), 8.57 (dd, J = 4.8, 1.6 Hz, 2H, H-4), 7.90 (dt, J = 7.9, 1.9 Hz, 2H, H-6), 7.76 (br t, J = 1.4 Hz, 1H, H-12), 7.61 (dd, J = 7.7, 1.7 Hz, 2H, H-10), 7.48 (t, J = 7.7 Hz, 1H, H-11), 7.39 (ddd, J = 7.9, 4.8, 0.7 Hz, 2H, H-5); ^{13}C (125 MHz): δ 153.0 (C-2), 150.1 (C-4), 139.4 (C-6), 135.2 (C-12), 132.9 (C-10), 130.3 (C-11), 124.4 (C-5), 124.1 (C-9), 120.7 (C-1) 91.9 (C-8), 87.7 (C-7) ppm; HR-ESI MS (DCM/MeOH): m/z 331.122 ($[\mathbf{L_4}+H]^+$, calcd for $C_{24}H_{15}N_2$ 331.123), 353.103 ($[\mathbf{L_4}+Na]^+$, calcd for $C_{24}H_{14}N_2Na$ 353.105); Anal. Calcd for $C_{20}H_{12}N_2 \cdot 0.25(H_2O)$ C 84.34, H 4.42, N 9.84. Found: C 84.61, H 4.55, N 9.49%

2,7-Bis(pyridin-3-ylethynyl)naphthalene, L_4. CuI (0.011 g, 0.06 mmol), $Pd(PPh_3)_2Cl_2$ (0.020 g, 0.03 mmol), 2,7-diethynylnaphthalene (0.050 g, 0.28 mmol), and 3-iodopyridine (0.116 g, 0.57 mmol) in THF (10 mL) and triethylamine (10 mL) to yield $\mathbf{L_4}$ as a pale yellow solid (0.071 g, 76%). Mp: 183−184 °C; IR (ATR): $\bar{\nu}$ 1557, 1503, 1472, 1437, 1405, 1188, 1119, 1020, 955, 916, 840, 808, 754, 720, 699, 624, 596, 540, 502, 478, 403 cm^{-1}; ^1H NMR (500 MHz, $CDCl_3$): δ 8.83 (s, 2H, H-2), 8.58 (d, J = 4.9 Hz, 2H, H-4), 8.05 (s, 2H, H-14), 7.86 (d, J = 7.9 Hz, 2H, H-6), 7.83 (d, J = 8.6 Hz, 2H, H-11), 7.62 (d, J = 8.6 Hz, 2H, H-10), 7.32 (dd, J = 7.9, 4.9 Hz, 2H, H-5); ^{13}C (125 MHz): δ 152.5 (C-2), 148.9 (C-4), 138.7 (C-6), 132.7 (C-12 and C-13), 131.7 (C-14), 129.5 (C-10), 128.3 (C-11), 123.3 (C-5), 121.0 (C-9), 120.5 (C-1), 92.8 (C-8), 87.0 (C-7) ppm; HR-ESI MS (DCM/MeOH): m/z 331.122 ($[\mathbf{L_4}+H]^+$, calcd for $C_{24}H_{15}N_2$ 331.123), 353.103 ($[\mathbf{L_4}+Na]^+$, calcd for $C_{24}H_{14}N_2Na$ 353.105); Anal. Calcd for $C_{24}H_{14}N_2$: C 87.25, H 4.27, N 8.48. Found: C 87.12, H 4.39, N 8.30%

2,6-Bis(pyridin-3-ylethynyl)pyridine, L_5. CuI (0.060 g, 0.32 mmol), $Pd(PPh_3)_2Cl_2$ (0.110 g, 0.16 mmol), 2,6-diethynylpyridine (0.200 g, 1.57 mmol) and 3-iodopyridine (0.645 g, 3.15 mmol) in THF (15 mL) and triethylamine (15 mL) to yield $\mathbf{L_5}$ as a pale yellow solid (0.357 g, 81%). Mp: 124 °C; IR (ATR): $\bar{\nu}$ 3035, 2221, 1555, 1476, 1439, 1406, 1290, 1239, 1188, 1165, 1122, 1021, 982, 797, 732, 698, 629, 527, 438, 402 cm^{-1}; ^1H NMR (500 MHz, $CDCl_3$): δ 8.84 (dd, J = 2.0, 0.8 Hz, 2H, H-2), 8.61 (dd, J = 4.9, 2.0 Hz, 2H, H-4), 7.89 (dt, J = 7.9, 2.0 Hz, 2H, H-6), 7.74 (dd, J = 7.8, 8.0 Hz, 1H, H-11), 7.54 (d, J = 7.8 Hz, 2H, H-10), 7.32 (ddd, J = 7.9, 4.9, 0.8 Hz, 2H, H-5); ^{13}C (125 MHz): δ 152.82 (C-2), 149.59 (C-4), 143.49 (C-9), 139.12 (C-6), 136.88 (C-11), 126.91 (C-10), 123.26 (C-5), 119.42 (C-1), 91.24 (C-8), 86.42 (C-7) ppm; HR-ESI MS (DCM/MeOH): m/z 282.109 ($[\mathbf{L_5}+H]^+$, calcd for $C_{19}H_{12}N_3$ 282.103), 304.084 ($[\mathbf{L_5}+Na]^+$, calcd for $C_{19}H_{11}N_3Na$ 304.085). Anal. Calcd for $C_{19}H_{11}N_3$ C 81.12, H 3.94, N 14.94. Found: C 80.85, H 3.95, N 14.66%

General Procedure for the Preparation of Silver Complexes of L_1, L_2, L_3, L_4, and L_5. To a solution of the ligand in acetone, a molar equivalent of the silver salt in acetone was added dropwise. The solution was stirred in the dark for 30 min during which time a white precipitate formed. This solid was isolated by filtration and was washed with diethyl ether to yield the silver complex.

Caution! *Although no problems were encountered with this work, perchlorate salts of metal complexes containing organic ligands are potentially explosive and should be handled with care and in small quantities.*

$\{[\mathbf{L_1}Ag](SbF_6)\}_n$. $\mathbf{L_1}$ (25 mg, 0.12 mmol) and $AgSbF_6$ (42 mg, 0.12 mmol) in acetone (10 mL) to give 61 mg (91%) of $\{[\mathbf{L_1}Ag](SbF_6)\}_n$. Mp: > 190 °C (decomp.); IR (ATR): $\bar{\nu}$ 1700, 1595, 1479, 1417, 1196, 820, 806, 691, 654, 636, 617 (br) cm^{-1}; ^1H NMR (400 MHz, d_6-acetone): δ 8.99 (dd, J = 2.1, 0.8 Hz, 2H, H-2), 8.80 (dd, J = 5.2, 1.6 Hz, 2H, H-4), 8.25 (dt, J = 8.0, 3.7 Hz, 2H, H-6), 7.71 (ddd, J = 8.0, 5.2, 0.8 Hz, 2H, H-5), ^{13}C (75 MHz,): δ 153.8 (C-2), 150.8 (C-4), 140.3 (C-6), 124.3 (C-5), 119.18 (C-1), 80.1 (C-7), 76.6 (C-8) ppm; HR-ESI MS (MeCN): m/z 310.970 ($[\mathbf{L_1}Ag]^+$, calcd for $C_{14}H_8N_2Ag$ 310.973), 515.036 ($[(\mathbf{L_1})_2Ag]^+$, calcd for $C_{28}H_{16}N_4Ag$ 515.042), 858.839 ($[(\mathbf{L_1})_2Ag_2SbF_6]^+$, calcd for $C_{28}H_{16}N_4Ag_2SbF_6$ 858.841), 1406.701 ($[(\mathbf{L_1})_3Ag_3(SbF_6)_2]^+$, calcd for $C_{42}H_{24}N_6Ag_3Sb_2F_{12}$ 1406.710), 1954.574 ($[(\mathbf{L_1})_4Ag_4(SbF_6)_3]^+$, calcd for $C_{56}H_{32}N_8Ag_4Sb_3F_{18}$ 1954.578); Anal. Calcd for $C_{14}H_8N_2F_6AgSb \cdot 0.25(C_3H_6O)$: C 31.50, H 1.70, N 4.98. Found: C 31.69, H 1.65, N 4.92%. X-ray

(38) Neenan, T. X.; Whitesides, G. M. *J. Org. Chem.* **1988**, *53*, 2489–2496.
(39) Dana, B. H.; Robinson, B. H.; Simpson, J. *J. Organomet. Chem.* **2002**, *648*, 251–269.

quality crystals with the formula $\{[\mathbf{L_1}Ag(CH_3CN)](SbF_6)\cdot CH_3CN\}_n$ were obtained by vapor diffusion of diethyl ether into an acetonitrile solution of $\{[\mathbf{L_1}Ag](SbF_6)\}_n$.

$\{[\mathbf{L_1}Ag](ClO_4)\}_n$. $\mathbf{L_1}$ (25 mg, 0.12 mmol) in acetone (2 mL) and $AgClO_4$ (25 mg, 0.12 mmol) in acetone (2 mL) to give 42 mg (83%) of $\{[\mathbf{L_1}Ag](ClO_4)\}_n$. HR-ESI MS (MeCN): *m/z*; 310.967 ($[\mathbf{L_1}Ag]^+$, calcd for $C_{14}H_8N_2Ag$ 310.973), 328.985 ($[\mathbf{L_1}Ag+H_2O]^+$, calcd for $C_{14}H_{10}N_2OAg$ 328.984), 515.033 ($[(\mathbf{L_1})_2Ag]^+$, calcd for $C_{28}H_{16}N_4Ag$ 515.042), 722.887 ($[(\mathbf{L_1})_2Ag_2ClO_4]^+$, calcd for $C_{28}H_{16}N_4Ag_2ClO_4$ 722.895); Anal. Calcd for $C_{14}H_8N_2O_4ClAg\cdot 0.25(C_3H_6O)$: C 41.58, H 2.25, N 6.57. Found: C 41.35, H 1.95, N 6.87%. X-ray quality crystals with the formula $\{[\mathbf{L_1}Ag(CH_3CN)](ClO_4)\}_n$ were obtained by vapor diffusion of diethyl ether into an acetonitrile solution of $\{[\mathbf{L_1}Ag](ClO_4)\}_n$.

$\{[\mathbf{L_1}Ag](BF_4)\}_n$. $\mathbf{L_1}$ (35 mg, 0.17 mmol) in acetone (2 mL) and $AgBF_4$ (33 mg, 0.17 mmol) in acetone (2 mL) to give $\{[\mathbf{L_1}Ag](BF_4)\}_n$ as a white solid (66 mg, 97%). Mp: > 210 °C; IR (ATR): $\bar{\nu}$ 1595, 1480, 1420, 1198, 1049 (br), 1025 (br), 807, 765, 693, 656, 518, 405 cm^{-1}; HR-ESI MS (MeCN): *m/z* 310.962 ($[\mathbf{L_1}Ag]^+$, calcd for $C_{14}H_8N_2Ag$ 310.973), 642.918 ($[(\mathbf{L_1})_2Ag_2F]^+$, calcd for $C_{28}H_{16}N_4Ag_2F$ 642.945), 710.923 ($[(\mathbf{L_1})_2Ag_2BF_4]^+$, calcd for $C_{28}H_{16}N_4Ag_2BF_4$ 710.950); Anal. Calcd for $C_{14}H_8N_2F_4BAg\cdot 0.5(H_2O)$: C 41.22, H 2.22, N 6.87. Found: C 41.54, H 1.98, N 6.61%.

$\{[\mathbf{L_1}Ag](SO_3CF_3)\}_n$. $\mathbf{L_1}$ (50 mg, 0.25 mmol) in acetone (2 mL) and $AgSO_3CF_3$ (63 mg, 0.25 mmol) in acetone (2 mL) to give 96 mg (85%) of $\{[\mathbf{L_1}Ag](SO_3CF_3)\}_n$. Mp: > 230 °C; IR (ATR): $\bar{\nu}$ 1593, 1472, 1419, 1271, 1236, 1221, 1196, 1170, 1051, 1022, 811, 696, 633, 573, 515, 408 cm^{-1}; HR-ESI MS (MeCN): *m/z* 310.968 ($[\mathbf{L_1}Ag]^+$, calcd for $C_{14}H_8N_2Ag$ 310.973), 515.029 ($[(\mathbf{L_1})_2Ag]^+$, calcd for $C_{28}H_{16}N_4Ag$ 515.042), 772.882 ($[(\mathbf{L_1})_2Ag_2SO_3CF_3]^+$, calcd for $C_{29}H_{16}N_4Ag_2SO_3F_3$ 772.889); Anal. Calcd for $C_{15}H_8N_2O_3F_3SAg\cdot 0.25(H_2O)$: C 38.69, H 1.84, N 6.02. Found: C 38.52, H 1.75, N 5.90%.

$\{[\mathbf{L_2}Ag](SbF_6)\}_n$. $\mathbf{L_2}$ (50 mg, 0.18 mmol) in acetone (2 mL) and $AgSbF_6$ (61 mg, 0.18 mmol) in acetone (2 mL) to give 55 mg (49%) of $\{[\mathbf{L_2}Ag](SbF_6)\}_n$. Mp: > 230 °C; IR (ATR): $\bar{\nu}$ 2226, 1598, 1572, 1510, 1419, 1196, 1158, 1125, 1102, 838, 807, 695, 654, 548, 409 cm^{-1}; ^1H NMR (500 MHz, d_6-acetone): δ 8.86 (d, J = 1.7 Hz, 2H, H-2), 8.69 (dd, J = 4.9, 1.4 Hz, 2H, H-4), 8.09 (dt, J = 7.9, 1.7 Hz, 2H, H-6), 7.67 (s, 4H, H-10), 7.59 (dd, J = 7.9, 4.9 Hz, 2H, H-5) ppm; HR-ESI MS(MeCN) *m/z*; 386.997 ($[\mathbf{L_2}Ag]^+$, calcd for $C_{20}H_{12}N_2Ag$ 387.005), 405.008 ($[\mathbf{L_2}Ag+H_2O]^+$, calcd for $C_{20}H_{14}N_2OAg$ 405.015), 669.085 ($[(\mathbf{L_2})_2Ag]^+$, calcd for $C_{40}H_{24}N_4Ag$ 669.105); Anal. Calcd for $C_{20}H_{12}N_2F_6AgSb$: C 38.50, H 1.94, N 4.49. Found: C 38.84, H 1.92, N 4.37%.

$\{[\mathbf{L_2}Ag](ClO_4)\}_n$. $\mathbf{L_2}$ (50 mg, 0.18 mmol) in acetone (2 mL) and $AgClO_4$ (37 mg, 0.25 mmol) in acetone (2 mL) to give 83 mg (95%) of $\{[\mathbf{L_2}Ag](ClO_4)\}_n$. HR-ESI MS (MeCN): *m/z* 387.002 ($[\mathbf{L_2}Ag]^+$, calcd for $C_{20}H_{12}N_2Ag$ 387.005), 388.005 ($[(\mathbf{L_2})_2Ag_2]^{2+}$, calcd for $C_{40}H_{24}N_4Ag_2$ 388.005), 405.012 ($[\mathbf{L_2}Ag+H_2O]^+$, calcd for $C_{20}H_{14}N_2OAg$ 405.015), 669.097 ($[(\mathbf{L_2})_2Ag]^+$, calcd for $C_{40}H_{24}N_4Ag$ 669.105); Anal. Calcd for $C_{20}H_{12}N_2O_4ClAg\cdot 0.5(H_2O)$: C 48.37, H 2.64, N 5.64. Found: C 48.35, H 2.67, N 5.34%.

$\{[\mathbf{L_2}Ag](BF_4)]\}_n$. $\mathbf{L_2}$ (50 mg, 0.18 mmol) in acetone (5 mL) and $AgBF_4$ (35 mg, 0.18 mmol) in acetone (5 mL) to give 71 mg (84%) $\{[\mathbf{L_2}Ag](BF_4)]\}_n$. Mp: > 210 °C; IR (ATR): $\bar{\nu}$ 2226, 1597, 1572, 1509, 1479, 1419, 1198, 1049 (br), 836, 807, 695, 654, 548, 533, 518, 495, 419 cm^{-1}; HR-ESI MS (MeCN): *m/z*; 386.994 ($[\mathbf{L_2}Ag]^+$, calcd for $C_{20}H_{12}N_2Ag$ 387.005), 405.004 ($[\mathbf{L_2}Ag+H_2O]^+$, calcd for $C_{20}H_{14}N_2OAg$ 405.015), 669.079 ($[(\mathbf{L_2})_2Ag]^+$, calcd for $C_{40}H_{24}N_4Ag$ 669.105); Anal. Calcd for $C_{20}H_{12}N_2AgBF_4\cdot H_2O$: C 48.72, H 2.86, N 5.68. Found: C 48.89, H 2.54, N 5.30%.

$\{[\mathbf{L_2}Ag](SO_3CF_3)\}_n$. $\mathbf{L_2}$ (50 mg, 0.18 mmol) in acetone (10 mL) and $AgSO_3CF_3$ (46 mg, 0.18 mmol) in acetone (2 mL) to give 55 mg (57%) of $\{[\mathbf{L_2}Ag](SO_3CF_3)\}_n$. Mp: > 210 °C; IR (ATR): $\bar{\nu}$ 2225, 1596, 1572, 1511, 1419, 1276, 1237, 1197, 1159, 1024, 832, 806, 694, 634, 547 cm^{-1}; HR-ESI MS (MeCN): *m/z*; 386.995 ($[\mathbf{L_2}Ag]^+$, calcd for $C_{20}H_{12}N_2Ag$ 387.005), 405.005 ($[\mathbf{L_2}Ag+H_2O]^+$, calcd for $C_{20}H_{14}N_2OAg$ 405.015), 669.081 ($[(\mathbf{L_2})_2Ag]^+$, calcd for $C_{40}H_{24}N_4Ag$ 669.105), 924.931 ($[(\mathbf{L_2})_2Ag_2O_3SCF_3]^+$, calcd for $C_{40}H_{24}N_4O_3SF_3Ag$ 924.962); Anal. Calcd for $C_{21}H_{12}F_3N_2O_3SAg$ C 46.95, H 2.25, N 5.21. Found: C 47.17, H 2.19, N 4.83%.

$[(\mathbf{L_3})_2Ag_2](SbF_6)_2$. $\mathbf{L_3}$ (56 mg, 0.20 mmol) in acetone (8 mL) and $AgSbF_6$ (69 mg, 0.20 mmol) in acetone (2 mL) to give 114 mg (91%) of $[(\mathbf{L_3})_2Ag_2](SbF_6)_2$. Mp: > 205 °C (decomp.); IR (ATR) $\bar{\nu}$ 2218, 1600, 1571, 1486, 1418, 1198, 1126, 1098, 1055, 1031, 797, 694, 684, 653 cm^{-1}; ^1H NMR (500 MHz, d_6-acetone): δ 8.95 (s, 2H, H-2), 8.73 (d, J = 5.0 Hz, 2H, H-4), 8.17 (dt, J = 8.0, 1.7 Hz, 2H, H-6), 7.78 (s, 1H, H-12), 7.70 (d, J = 7.6 Hz, 2H, H-10), 7.67 (dd, J = 7.0, 5.0 Hz, 2H, H-5), 7.58 (t, J = 7.6 Hz, 1H, H-11); ^{13}C (125 MHz): δ 154.0 (C-2), 151.1 (C-4), 141.0 (C-6), 135.2 (C-12), 133.2 (C-10), 130.4 (C-11), 125.5 (C-5), 123.8 (C-9), 121.7 (C-1), 92.7 (C-8), 86.8 (C-7) ppm; HR-ESI MS (MeCN): *m/z* 387.006 ($[\mathbf{L_3}Ag]^+$, calcd for $C_{20}H_{12}N_2Ag$ 387.005), 1010.904 ($[(\mathbf{L_3})_2Ag_2SbF_6]^+$, calcd for $C_{40}H_{24}N_4F_6SbAg_2$ 1010.904), 1634.802 ($[(\mathbf{L_3})_3Ag_3(SbF_6)_2]^+$, calcd for $C_{60}H_{36}N_6F_{12}Sb_2Ag_3$ 1634.804), 2258.711 ($[(\mathbf{L_3})_4Ag_4(SbF_6)_3]^+$, calcd for $C_{80}H_{48}N_8F_{18}Sb_3Ag_4$ 2258.704); Anal. Calcd for $C_{40}H_{24}Ag_2N_4Sb_2F_{12}$: C 38.50, H 1.94, N 4.49. Found: C 38.61, H 2.13, N 4.43%.

$[(\mathbf{L_3})_2Ag_2](ClO_4)_2$. $\mathbf{L_3}$ (56 mg, 0.20 mmol) in acetone (8 mL) and $AgClO_4$ (41 mg, 0.20 mmol) in acetone (2 mL) to give 144 mg (73%) of $[(\mathbf{L_3})_2Ag_2](ClO_4)_2$. HR ESI MS (MeCN): *m/z* 387.008 ($[\mathbf{L_3}Ag]^+$, calcd for $C_{20}H_{12}N_2Ag$ 387.005), 387.008 ($[(\mathbf{L3})_2Ag_2]^{2+}$, calcd for $C_{40}H_{24}N_4Ag_2$ 387.005), 669.102 ($[(\mathbf{L_3})_2Ag]^+$, calcd for $C_{40}H_{24}N_4Ag$ 669.105), 874.953 ($[(\mathbf{L_3})_2Ag_2ClO_4]^+$, calcd for $C_{40}H_{24}N_4O_4ClAg_2$ 874.958); Anal. Calcd for $C_{40}H_{24}AgClN_4O_8\cdot 0.5(C_3H_6O)$: C 49.98, H 2.93, N 5.42. Found: C 50.13, H 2.92, N 5.08%. X-ray quality crystals with the formula $[(\mathbf{L_3})_2Ag_2](ClO_4)_2\cdot 3H_2O$ were obtained by vapor diffusion of diethyl ether into an acetonitrile solution of $[(\mathbf{L_3})_2Ag_2](ClO_4)_2$.

$[(\mathbf{L_3})_2Ag_2](BF_4)_2$. $\mathbf{L_3}$ (50 mg, 0.18 mmol) in acetone (8 mL) and $AgBF_4$ (35 mg, 0.18 mmol) in acetone (2 mL) to give 56 mg (66%) of $[(\mathbf{L_3})_2Ag_2](BF_4)_2$. Mp: > 210 °C; IR (ATR) $\bar{\nu}$ 2220, 1632, 1598, 1417, 1023 (br), 795, 694, 683, 654, 520, 436 cm^{-1}; HR-ESI MS (MeCN): *m/z* 387.008 ($[\mathbf{L_3}Ag]^+$, calcd for $C_{20}H_{12}N_2Ag$ 387.005), 387.008 ($[(\mathbf{L3})_2Ag_2]^{2+}$, calcd for $C_{40}H_{24}N_4Ag_2$ 387.005), 669.104 ($[(\mathbf{L_3})_2Ag]^+$, calcd for $C_{40}H_{24}N_4Ag$ 669.105); Anal. Calcd for $C_{20}H_{12}N_2AgBF_4\cdot 0.5(H_2O)$: C 49.63, H 2.71, N 5.79. Found: C 49.71, H 2.63, N 5.55%.

$[(\mathbf{L_3})_2Ag_2](SO_3CF_3)_2$. $\mathbf{L_3}$ (56 mg, 0.20 mmol) in acetone (8 mL) and $AgSO_3CF_3$ (51 mg, 0.20 mmol) in acetone (2 mL) to give 81 mg (75%) of $[(\mathbf{L_3})_2Ag_2](SO_3CF_3)_2$. Mp: 205 °C; IR (ATR) $\bar{\nu}$ 2216, 1597 1569, 1483, 1414, 1250, 1163, 1026, 803, 697, 683, 636, 573, 517 cm^{-1}; HR-ESI MS (MeCN): *m/z* 387.008 ($[\mathbf{L_3}Ag]^+$, calcd for $C_{20}H_{12}N_2Ag$ 387.005), 644.865 ($[\mathbf{L_3}Ag_2SO_3CF_3]^+$, calcd for $C_{21}H_{12}N_2Ag_2F_3SO_3$ 644.862), 924.963 ($[(L_3)_2Ag_2SO_3CF_3]^+$, calcd for $C_{41}H_{24}N_4Ag_2F_3SO_3$ 924.962); Anal. Calcd for $C_{21}H_{12}AgN_2SO_3F_3$: C 46.95, H 2.25, N 5.21. Found: C 47.20, H 2.32, N 5.06%.

$[(\mathbf{L_4})_2Ag_2](SbF_6)_2$. $\mathbf{L_4}$ (20 mg, 0.06 mmol) in acetone (3 mL) and $AgSbF_6$ (21 mg, 0.06 mmol) in acetone (3 mL) to give 32 mg (79%) of $[(\mathbf{L_4})_2Ag_2](SbF_6)_2$. Mp: > 210 °C; IR (ATR) $\bar{\nu}$ 2216, 1592, 1571, 1505, 1482, 1418, 1367, 1226, 1196, 1055, 909, 847, 805, 693, 649, 487 cm^{-1}; HR-ESI MS (MeCN): *m/z* 769.140 ($[(\mathbf{L_4})_2Ag]^+$, calcd for $C_{48}H_{28}N_4Ag$ 769.136), 1110.941 ($[(\mathbf{L_4})_2Ag_2SbF_6]^+$, calcd for $C_{48}H_{28}N_4Ag_2SbF_6$ 1110.936); ^1H NMR (400 MHz, d_6-acetone): δ 8.95 (br s, 2H, H-2), 8.70 (br s, 2H, H-4), 8.23 (s, 2H, H-14), 8.13 (m, 2H, H-6), 8.04 (d, J = 8.4 Hz, 2H, H-11), 7.73 (dd, J = 8.4, 1.2 Hz, 2H, H-10), 7.62 (m, 2H, H-5) ppm; Anal. Calcd for $C_{48}H_{28}Ag_2N_4Sb_2F_{12}\cdot(C_3H_6O)$: C 43.56, H 2.44, N 3.98. Found: C 43.39, H 2.20, N 3.86%.

$[(\mathbf{L_4})_2Ag_2](ClO_4)_2$. $\mathbf{L_4}$ (20 mg, 0.06 mmol) in acetone (3 mL) and $AgClO_4$ (13 mg, 0.06 mmol) in acetone (3 mL) to give 28 mg

Table 1. Crystallographic Data for the Silver(I) Complexes

	$\{[\mathbf{L_1}Ag(CH_3CN)](ClO_4)\}_n$	$\{[\mathbf{L_1}Ag(CH_3CN)](SbF_6)\cdot CH_3CN\}_n$	$[(\mathbf{L_3})_2Ag_2](ClO_4)_2\cdot 3H_2O$	$\{[\mathbf{L_5}Ag](ClO_4)\cdot 0.5Et_2O\}_n$
CCDC depository	795010	795008	795011	795009
formula	$C_{16}H_{11}N_3O_4ClAg$	$C_{18}H_{14}N_4F_6AgSb$	$C_{20}H_{15}N_2O_{5.5}ClAg$	$C_{42}H_{32}N_6O_9Cl_2Ag_2$
formula weight	452.60	629.95	514.66	1051.38
T (K)	90	89	90	93
crystal system	orthorhombic	triclinic	triclinic	monoclinic
space group	*Pbca*	$P\bar{1}$	$P\bar{1}$	$P2_1/n$
a (Å)	14.4471(10)	7.623(5)	9.9203(25)	9.5050(10)
b (Å)	13.9583(11)	11.505(6)	10.8747(29)	13.797(2)
c (Å)	16.5272(13)	12.375(9)	11.6781(33)	16.3534(17)
α (deg)	90	92.43(2)	112.223(10)	90
β (deg)	90	99.992(11)	102.814(12)	97.151(5)
γ (deg)	90	92.46(3)	106.508(11)	90
V (Å^3)	3332.8(4)	1069.7(12)	1038.4(4)	2128.0(5)
Z	8	2	2	2
crystal size	0.40 × 0.21 × 0.12	0.21 × 0.15 × 0.06	0.84 × 0.26 × 0.12	0.53 × 0.15 × 0.10
ρ /g cm^3	1.804	1.956	1.646	1.641
μ/mm^{-1}	1.396	2.241	1.135	1.108
reflections collected	104979	13514	21794	11963
independent reflections (R_{int})	6084 (0.0465)	3669 (0.0722)	3745 (0.0345)	3572 (0.0480)
data/restraints/parameters	6084/0/227	3669/0/273	3745/0/253	3572/21/299
goodness of fit on F^2	1.047	1.019	1.089	1.077
final indexes [$I > 2\sigma$(I)]	$R_1 = 0.0254$	$R_1 = 0.0649$	$R_1 = 0.0350$	$R_1 = 0.0778$
	$wR_2 = 0.0580$	$wR_2 = 0.1645$	$wR_2 = 0.1025$	$wR_2 = 0.2091$
final indexes (all data)	$R_1 = 0.0380$	$R_1 = 0.0940$	$R_1 = 0.0370$	$R_1 = 0.0876$
	$wR_2 = 0.0622$	$wR_2 = 0.1856$	$wR_2 = 0.1051$	$wR_2 = 0.2144$
largest difference (e Å^{-3})	0.569 and −0.625	2.455 and −1.084	0.958 and −0.698	3.670 and −1.039

(87%) of $[(\mathbf{L_4})_2Ag_2](ClO_4)_2$. HR-ESI MS (MeCN): m/z 437.023 ($[\mathbf{L_4}Ag]^+$, calcd for $C_{24}H_{14}N_2Ag$ 437.020), 437.023 ($[(\mathbf{L_4})_2Ag_2]^{2+}$, calcd for $C_{48}H_{28}N_4Ag_2$ 437.020), 769.132 ($[(\mathbf{L_4})_2Ag]^+$, calcd for $C_{48}H_{28}N_4Ag$ 769.136), 974.991 ($[(\mathbf{L_4})_2Ag_2ClO_4]^+$, calcd for $C_{48}H_{28}N_4Ag_2ClO_4$ 974.989), 1512.965 ($[(\mathbf{L_4})_3Ag_3(ClO_4)_2]^+$, calcd for $C_{72}H_{42}N_6Ag_3Cl_2O_8$ 1512.959); Anal. Calcd for $C_{48}H_{28}Ag_2Cl_2N_4O_8\cdot(C_3H_6O)$: C 54.04, H 3.02, N 4.92. Found: C 54.07, H 3.19, N 4.52%.

$[(\mathbf{L_5})_2Ag_2](SbF_6)_2$. $\mathbf{L_5}$ (50 mg, 0.18 mmol) in acetone (3 mL) and $AgSbF_6$ (61 mg, 0.18 mmol) in acetone (3 mL) to give 101 mg (91%) of $[(\mathbf{L_5})_2Ag_2](SbF_6)_2$. Mp: >210 °C; IR (ATR): $\bar{\nu}$ 2232, 1582, 1557, 1482, 1450, 1415, 809, 697, 653 (br), 557 cm^{-1}; ^{1}H NMR (400 MHz, d_6-acetone): δ 8.97 (s, 2H, H-2), 8.76 (d, J = 5.3 Hz, 2H, H-4), 8.13 (m, 3H, H-6 and H-11), 7.87 (d, J = 8.0 Hz, 2H, H-10), 7.62 (dd, J = 7.9 and 5.3 Hz, 2H, H-5) ppm; HR-ESI MS (MeCN): m/z 387.998 ($[\mathbf{L_5}Ag]^+$, calcd for $C_{19}H_{11}N_3Ag$ 387.999), 671.091 ($[(\mathbf{L_5})_2Ag]^+$, calcd for $C_{38}H_{22}N_6Ag$ 671.095), 1012.887 ($[(\mathbf{L_5})_2Ag_2SbF_6]^+$, calcd for $C_{38}H_{22}Ag_2N_6SbF_6$ 1012.895), 1637.775 ($[(\mathbf{L_5})_3Ag_3(SbF_6)_2]^+$, calcd for $C_{57}H_{33}Ag_3N_9Sb_2F_{12}$ 1637.790); Anal. Calcd for $C_{38}H_{22}Ag_2N_6Sb_2F_{12}$: C 36.52, H 1.77, N 6.72. Found: C 36.44, H 1.76, N 6.65%.

$[(\mathbf{L_5})_2Ag_2](ClO_4)_2$. $\mathbf{L_5}$ (50 mg, 0.18 mmol) in acetone (3 mL) and $AgClO_4$ (37 mg, 0.18 mmol) in acetone (3 mL) to give 76 mg (87%) of $[(\mathbf{L_5})_2Ag_2](ClO_4)_2$. HR-ESI MS (MeCN): m/z 671.108 ($[(L_5)_2Ag]^+$, calcd for $C_{38}H_{22}N_6Ag$ 671.095); Anal. Calcd for $C_{38}H_{22}N_6O_8Cl_2Ag_2$: C 46.70, H 2.28, N 8.60. Found: C 46.86, H 2.28, N 8.55%. X-ray quality crystals with the formula $\{[(\mathbf{L_5})_2Ag_2](ClO_4)_2\cdot Et_2O\}_n$ were obtained by vapor diffusion of diethyl ether into an acetonitrile solution of $[(\mathbf{L_5})_2Ag_2](ClO_4)_2$.

X-ray Data Collection and Refinement. X-ray data for $[(\mathbf{L_3})_2Ag_2](ClO_4)_2\cdot 3H_2O$, $\{[(\mathbf{L_5})Ag](ClO_4)\cdot 0.5Et_2O\}_n$, $\{[(\mathbf{L_1})Ag(CH_3CN)](ClO_4)\}_n$, $\{[(\mathbf{L_1})Ag(CH_3CN)](SbF_6)\cdot CH_3CN\}_n$ were recorded with a Bruker APEX II CCD diffractometer at 90(2) or 89(2) K using Mo−Kα radiation (λ = 0.71073 Å). The structures were solved by direct methods using SIR97[40] with the resulting Fourier maps revealing the location of all non-hydrogen atoms. Weighted full-matrix least-squares refinements on F^2 were carried out using SHELXL-97[41] with all non-hydrogen atoms being refined anisotropically. The hydrogen atoms were included in calculated positions and were refined as riding atoms with individual (or group, if appropriate) isotropic displacement parameters.

In the structure $[(\mathbf{L_3})_2Ag_2](ClO_4)_2\cdot 3H_2O$, the channels formed by the slip-stacked Ag-pyridylalkyne rings are filled with disordered water molecules. Four discrete sites with partial occupancy accounted for most of the electron density in these channels, so that the largest residual peaks of electron density were concentrated near the silver center. However, the model that led to the lowest values for R_1 and wR_2 (0.037 and 0.107, respectively) lacked chemical sense (3 sites within 2 Å, each having 0.5 occupancy) and atoms had highly eccentric ellipsoids for the atomic displacement parameters. The SQUEEZE[42] routine of PLATON revealed 24 electrons or approximately 3 water molecules per unit cell. Crystal data and collection parameters are given in Table 1. CCDC 795008−795011 contain the supplementary crystallographic data for this paper. These data can be obtained free of charge from the Cambridge Crystallographic Data Centre via www.ccdc.cam.ac.uk/data_request/cif

Conclusions

We have synthesized and characterized a family of planar di- and tri-silver(I) metallo-macrocycles. The silver(I) complexes have been fully characterized by elemental analysis, HR-ESI-MS, IR, ^{1}H and ^{13}C NMR spectroscopy, and the solution data are consistent with the formation of the metallo-macrocycles. However, X-ray crystallography shows that only one of the silver(I) complexes maintains its macrocyclic structure in the solid state. This di-silver(I) macrocycle assembles into a nanoporous chicken-wire like structure in which the pores are filled with ClO_4^- and disordered H_2O molecules. The lability of the silver(I) ions enables the other macrocyclic complexes to ring-open and crystallize as nonporous coordination polymers. In combination these results

(40) Altomare, A.; Burla, M. C.; Camalli, M.; Cascarano, G. L.; Giacovazzo, C.; Guagliardi, A.; Moliterni, A. G. G.; Polidori, G.; Spagna, R. *J. Appl. Crystallogr.* **1999**, *32*, 115–119.

(41) Sheldrick, G. M.; Schneider, T. R. *Methods Enzymol.* **1997**, *277*, 319–343. Sheldrick, G. M. *Acta Crystallogr., Sect. A: Found. Crystallogr.* **2008**, *A64*, 112–122.

(42) Spek, A. L. *J. Appl. Crystallogr.* **2003**, *36*, 7–13.

suggest that the cationic planar silver(I) metallo-macrocycles are not suitable building blocks for the self-assembly of linear metal−organic nanotubes. In light of this we are now investigating second-generation neutral planar metallo-macrocycles of less labile metal ions such as Au(I) and Pt(II).

Acknowledgment. We thank Dr. Mervyn Thomas for his assistance collecting NMR data and Dr. David McMorran for useful discussions. A University of Otago Research Grant and the Department of Chemistry, University of Otago provided financial support for this work. The MacDiarmid Institute for Advanced Materials and Nanotechnology is thanked for providing funding for the purchase of X-ray optics and a detector and the Allan Wilson Centre for Molecular Ecology and Evolution for the purchase of the microfocus rotating-anode X-ray generator.

Supporting Information Available: X-ray crystallographic data for $\{[\mathbf{L_1}Ag(CH_3CN)](ClO_4)\}_n$, $\{[\mathbf{L_1}Ag(CH_3CN)](SbF_6)\cdot CH_3CN\}_n$, $[(\mathbf{L_3})_2Ag_2](ClO_4)_2\cdot 3H_2O$, and $\{[\mathbf{L_5}Ag](ClO_4)\cdot 0.5Et_2O\}_n$ in CIF format. NMR and ESI-MS data, molecular modelling and crystal-packing diagrams are also available. This material is available free of charge via the Internet at http://pubs.acs.org.